

Dynamic Games of Asymmetric Information for Deceptive Autonomous Vehicles

Linan Huang, *Student Member, IEEE*, Quanyan Zhu, *Member, IEEE*

Abstract

This paper studies rational and persistent deception among intelligent robots to enhance the security and operation efficiency of autonomous vehicles. We present an N -person K -stage nonzero-sum game with an asymmetric information structure where each robot's private information is modeled as a random variable or its type. The deception is persistent as each robot's private type remains unknown to other robots for all stages. The deception is rational as robots aim to achieve their deception goals at minimum cost. Each robot forms a belief on others' types based on state observations and updates it via the Bayesian rule. The level- t perfect Bayesian Nash equilibrium is a natural solution concept of the dynamic game. It demonstrates the sequential rationality of the agents, maintains the belief consistency with the observations and strategies, and provides a reliable prediction of the outcome of the deception game. In particular, in the linear-quadratic setting, we derive a set of extended Riccati equations, obtain the explicit form of the affine state-feedback control, and develop an online computational algorithm. We define the concepts of deceivability and the price of deception to evaluate the strategy design and assess the deception outcome. We investigate a case study of deceptive pursuit-evasion games and use numerical experiments to corroborate the results.

Index Terms

Game theory, deception, linear-quadratic control, pursuit-evasion games, Nash equilibrium

I. INTRODUCTION

DECEPTION is a ubiquitous phenomenon in the biological world [1], military [2], politics and media [3], and cyberspace [4]. In particular, deception plays an increasingly significant role in artificial intelligence and robotic systems. The recent advances in autonomous vehicles and smart robot technologies have not only allowed them to adapt to the dynamic environment via real-time observations, but also made them easily deceivable. The deceiver can intentionally hide or reveal selected information to alter the belief and behavior of the target robots for a higher reward. Since deception has various forms and delivery methods, understanding deception in a unified and quantitative framework is an indispensable step toward assessing the outcomes, measuring the impact, and designing strategies. This work aims to design robots that can interact with others efficiently under deceptive environments.

We identify the following challenges and features of robot deception. First, by definition, deception involves at least two participants interacting with each other. An intelligent robot should further consider other participants' rationality, predict their potential deceptive behaviors, and adjust its behaviors accordingly to alleviate the negative effect of deception. Second, due to the robots' dynamic nature, one-shot deception can exert a subsequent influence. Thus, the participating robots need to form long-term objectives to deceive or counter-deceive other robots. The multi-stage interactions also make it possible for the deceiver to apply deception at different stages. Third, each robot contains heterogeneous private information, which results in an asymmetric cognition structure; i.e., robots can form different beliefs over the same piece of unknown information. Thus, besides the couplings of state dynamics and costs, the multi-agent system further has the cognition coupling; i.e., each robot's behaviors are not only affected by its own belief but also the beliefs of the others.

To capture these features, we model the deceptive interaction between N strategic robots as a K -stage game of incomplete information. During the finite K stages, N robots accomplish non-cooperative tasks such as pursuit-evasion in the battlefield [5] or cooperative tasks such as collective towing [6], [7]. Robots introduce deception in the above interacting scenarios due to antagonism, selfishness, and privacy concerns. Following Harsanyi's approach [8], we capture each robot's private information using a random variable. The realization of the random variable,

which is called the type of the robot, is known only to itself, while the support of the random variable, which contains all its possible types, is known to all robots. Take the pursuit-evasion scenario as an example, due to the constraints of weather, terrain, and weapon, both the evading and the pursuing robots know the feasible beachheads for the evader to land on. However, the evader chooses only one beachhead as his private and confidential decision, known as the type. Other robots such as the pursuer in the battlefield know the existence of the deception and apply Bayesian learning to counter the deception; i.e., they form and update their beliefs based on real-time observations. Since these tasks are usually time-constrained, robots cannot wait until they have learned the true type. Instead, they have to take concurrent actions while the deceiver's type remains uncertain.

Each robot aims to minimize its own expected cumulative costs over K stages. Since the expectation involves its belief of other players' private types, its actions should be consistent with the beliefs. Robots with the perfect belief consistency can determine their K -stage actions at the initial stage considering the potential belief updates for all future stages. Robots with the bounded belief consistency determine their next-stage actions at each stage assuming that the beliefs in the future stages are the same as the one at the current stage. Based on different belief consistency levels of participating robots, we define the corresponding Bayesian Nash Equilibrium (BNE). The BNE provides a reliable prediction of the outcome of the deception under rational behaviors because a unilateral deviation does not benefit those who deviate from the equilibrium.

We focus on a class of linear-quadratic problems to obtain the equilibrium policies in closed form, which are unique and take the form of the affine state-feedback. Moreover, we obtain a set of extended Riccati equations which explicitly characterize the coupling of the state dynamics, cost, and cognition of all robots. Under proper decoupling, the extended Riccati equations degenerate to the classical Riccati equations for the problems of optimal control and dynamic game of complete information. We define the Price of Deception (PoD) as a crucial metric of assessment and design for robot deception.

Finally, we propose a case study of dynamic target protection where an evader aims to deceptively reach one of the possible targets and simultaneously evade the pursuer. The game has doubled-sided asymmetric information. The evader's private or hidden information is his true target while the pursuer's private information is her capability to maneuver or the maneuverability. We propose multi-dimensional metrics including the stage of truth revelation and the endpoint distance to assess the deception impact. We define the concept of deceivability to characterize the fundamental limits of deception and investigate how it is affected by the distinguishability of the private information. We compare the proposed policy with two heuristic policies to demonstrate its efficiency under deception. We show that Bayesian learning can largely reduce the impact of initial belief manipulation and result in a win-win situation for some cases. The increase of the pursuer's maneuverability improves her control performance under deception yet has a marginal effect. We also find that applying deception to counter deception is not always effective; e.g., it can be beneficial for a low-maneuverability pursuer to disguise as a high-maneuverability pursuer but not vice versa.

A. Related Works

The secure and efficient operation of robots, autonomous vehicles, and industrial control systems is vital for recent advances in technologies. Many works [9]–[11] have investigated how to protect effectively these systems from attacks on measurements [12], communication channels [13], and control signals [14]. Deception is a key feature of sophisticated attacks with a focus on intentionally hiding private information, introducing randomness [15], and manipulating other players' beliefs [16]. Deception in robotic systems can be conducted through visual displays [17], facial expressions and body gestures [18], and trajectories [15], [19]. Existing works on robot deception are largely based on experimental approaches [15], [20], [21]. There is a need for a formal and quantitative framework to assess the deception impact, understand fundamental limits and tradeoffs of deception, and determine real-time strategies.

Game models such as hypergames [22], signaling games [23], dynamic Bayesian games [24], and partially observable Markov games [25] have been adopted as natural analytic paradigms to understand deception between intelligent players. Computation of the equilibrium solutions for dynamic games of incomplete information is often viewed as a challenging task. It is more so in the context of robotic systems where systems are constrained by physical dynamics. In this work, we adopt a receding horizon approach to compute Nash strategies, which yields computationally tractable online strategies for the players. Similar approaches have been used in other contexts including industrial control systems [26], [27], military air operation [28], and autonomous racing [29].

1) *Non-classical Information Structure*: We model deception by a non-classical structure of incomplete information [30]. Non-classical information structures can be classified into three categories, i.e., common information [31]; asymmetric information without information sharing [32]; asymmetric information with a sharing of the noisy state observation [33], the local state of sub-system [34], or the control input [35]. Our work falls into the third category where players have both common observations of the system states and private observation of their own types. In the third category, if each player further has the same objective function and the set of the common observation is finite, [36] has proposed the common-information approach to reduce the computation complexity.

2) *Bayesian Games and Signaling Effects*: Bayesian learning has been assimilated into stochastic control to deal with uncertainty, which induces the subgame perfect and the Markov perfect equilibrium for common information game [31] and perfect Bayesian equilibrium in the asymmetric information game such as signaling games and multi-stage games [37]. In these games, players make their decisions based on the belief profile and the belief can be strategy-independent [33] with no signaling effects, or strategy-dependent [32], [34] with a signaling effect. As discussed in Section 6 of [33], the signaling effect can result in an incentive to deceive. In our framework, players update their beliefs based on the observation of the system state, which is affected by all players' control strategies. Thus, players can change their control strategies to manipulate other players' beliefs to deceive and counter deception.

3) *Markov Jump System*: Our model has a connection with the discrete-time Markov jump system [38] as the jump system also involves a random variable called the *mode* whose realization is not observable throughout the stages. However, there are two differences. First, the mode jumps at each stage according to a known probabilistic transition kernel to model abrupt changes of the state dynamics. Players cannot apply the Bayesian update to learn the mode which changes continuously. Second, the mode uncertainty is caused by noise but the incomplete information of types in our model is introduced by strategic and deceptive players. If the state is further not directly observable, state estimation under jump mode via stochastic sampling [39] and particle filters [40] is also required.

B. Notations and Organization of the Paper

We summarize notations and variables in Table I. Calligraphic letter \mathcal{A} defines a set and $|\mathcal{A}|$ represents its cardinality. Define $\mathcal{B} \setminus \mathcal{A}$ as the set of elements in \mathcal{B} but not in \mathcal{A} . The indicator function $\mathbf{1}_{\{x=y\}}$ equals one when $x = y$, and zero otherwise. Let $\mathbb{E}_{a \sim A}[f(a)]$ denote the expectation of $f(a)$ over random variable a whose probability distribution is A . Denote Tr as the trace of the matrix and $'$ as the matrix transpose. Define $\{a_i\}_{i \in \mathcal{N}} := \{a_1, \dots, a_N\}$ as the set with N elements a_1, \dots, a_N , $[a_i]_{i \in \mathcal{N}} := [a_1, \dots, a_N]$ as N blocks arranged in a row, and $[a_1; \dots; a_N]$ as N blocks arranged in a column. Notation $\text{Diag}[a_1, \dots, a_N]$ represents (non-square) block diagonal matrix with diagonal blocks $a_i, i \in \mathcal{N}$, of any dimensions and $\mathbf{I}_w, \mathbf{0}_{m,n}$ are $w \times w$ identity matrix and $m \times n$ zero matrix, respectively. The superscript $k \in \mathcal{K}$ is the stage index and the subscript $i \in \mathcal{N}$ is the player index. We omit arguments of a function when there is no ambiguity; e.g., $S_i^k := S_i^k(I_i^k, \theta_i)$.

The rest of paper is organized as follows. Section II introduces the dynamic game with incomplete information and Bayesian Nash equilibrium concepts. To obtain explicit and practical solutions, we consider a class of a linear-quadratic problems in Section III and obtain a set of extended Riccati equations. We present a case study of deceptive pursuit-evasion in Section IV and Section V concludes the paper.

II. GENERAL FRAMEWORK

This section introduces a K -stage game consisting of N robots as players, which models deception as a dynamic process with asymmetric information among the players. Let $\mathcal{N} := \{1, \dots, N\}$ be the set of players and $\mathcal{K} := \{0, 1, 2, \dots, K\}$ be the set of K discrete stages. Private information of player $i \in \mathcal{N}$, i.e., type θ_i , is modeled as the realization of a discrete random variable with a finite support $\Theta_i := \{\theta_i^1, \theta_i^2, \dots, \theta_i^{N_i}\}$ where N_i is the number of possible types for player i . Each player i knows the value of his own type θ_i , but does not know the values of other players' types $\theta_{-i} := \{\theta_j\}_{j \in \mathcal{N} \setminus \{i\}} \in \Theta_{-i}$, throughout K stages of the game. Each set Θ_i is assumed to be *common knowledge*; i.e., all players know it, all players know that all players know it, and so on ad infinitum. The system state dynamics under N players' joint action $u^k := \{u_1^k, \dots, u_N^k\}$, joint type $\theta := \{\theta_1, \dots, \theta_N\}$, and an additive noise $w^k \in \mathbb{R}^{n \times 1}$ is shown in (1):

$$x^{k+1} = f^k(x^k, u_1^k, \dots, u_N^k, \theta_1, \dots, \theta_N) + w^k, k \in \mathcal{K} \setminus \{K\}. \quad (1)$$

TABLE I: Summary of notations and variables.

General Notation	Meaning
$\mathbf{1}_{\{x=y\}}$	Indicator function which equals one when $x=y$, and zero otherwise
$\{a_i\}_{i \in \mathcal{N}} := \{a_1, \dots, a_N\}$	Set with N elements a_1, \dots, a_N
$[a_i]_{i \in \mathcal{N}} := [a_1, \dots, a_N]$	N blocks arranged in a row
$[a_1; \dots; a_N]$	N blocks arranged in a column
$\text{Diag}[a_1, \dots, a_N]$	(Non-square) block diagonal matrix with diagonal blocks $a_i, i \in \mathcal{N}$, of any dimensions
$\mathbf{I}_w, \mathbf{0}_{m,n}$	$w \times w$ identity matrix and $m \times n$ zero matrix
Variable	Meaning
$\mathcal{N} := \{1, 2, \dots, N\}$	Set of N players in the dynamic game
$\Theta_i := \{\theta_i^1, \theta_i^2, \dots, \theta_i^{N_i}\}$	Set of N_i possible types for player $i \in \mathcal{N}$
$\theta_i \in \Theta_i$	Type of player $i \in \mathcal{N}$
$\Theta := \{\theta_1, \dots, \theta_N\}$	N players' joint type
$\Theta_{-i} := \{\theta_j\}_{j \in \mathcal{N} \setminus \{i\}}$	Types of all players except for player $i \in \mathcal{N}$
$\Theta_{-i} := \prod_{j \in \mathcal{N} \setminus \{i\}} \Theta_j$	Set of types of all players except for player i
$\Delta(\Theta_{-i})$	Set of probability distributions over set Θ_{-i}
$\mathcal{K} := \{0, 1, 2, \dots, K\}$	Set of K discrete stages in the dynamic game
$k, k_0 \in \mathcal{K}$	Index of stage k and index for the initial stage k_0
$x^k \in \mathbb{R}^{n \times 1}$	System state of dimension n at stage k
$x_i^k \in \mathbb{R}^{n_i \times 1}$	Player i 's state of dimension n_i at stage k
$u_i^k \in \mathbb{R}^{m_i \times 1}$	Player i 's action of dimension m_i at stage k
$u^k := \{u_1^k, \dots, u_N^k\}$	N players' joint action at stage k
$u_{-i}^k := \{u_j^k\}_{j \in \mathcal{N} \setminus \{i\}}$	Actions of all players except for i at stage k
$u_i^{k_0:K} := \{u_i^{k_0}, \dots, u_i^K\}$	Player i 's action sequence from stage k_0 to K
$u^{k_0:K} := \{u_i^{k_0:K}, u_{-i}^{k_0:K}\}$	Player i 's and all other players' control sequences from stage k_0 to K
f^k	State transition function at stage k
$h^k := \{x^0, \dots, x^k\} \in \mathcal{H}^k$	State history
$l_i^k(\theta_{-i} h^k, \theta_i)$	Player i 's belief at stage k , i.e., the probability of other players' type being θ_{-i} based on player i 's available information of h^k, θ_i

The dynamics in (1) can have different interpretations based on applications. In the pursuit-evasion scenario, e.g., [5], $x_i^k \in \mathbb{R}^{n_i \times 1}$ represents robot i 's local states such as its location and speed. The system state $x^k \in \mathbb{R}^{n \times 1}$ can be explicitly represented by N robots' joint state $\{x_1^k, \dots, x_N^k\}$ where $n = \sum_{i=1}^N n_i$. In the application where N robots cooperatively transport a payload, e.g., [6], [7], system state $x^k \in \mathbb{R}^{n \times 1}$ represents the payload's location and posture, which does not explicitly relate to robots' local states. The noise sequence $\{w^k\}_{k \in \mathcal{K}}$ is assumed to be independent with a known probability density function $d_w(\cdot)$; i.e., $\mathbb{E}_{w^l, w^j \sim d_w}[w^l(w^j)'] = 0, \forall l \neq j, l, j \in \mathcal{K}$. The noise is not necessarily Gaussian distributed but is assumed to have a zero mean and a covariance matrix Q^k ; i.e., $\mathbb{E}_{w^k \sim d_w}[w^k(w^k)'] = Q^k, \forall k \in \mathcal{K}$. We assume that the system dynamics f^k is multi-agent controllable as defined in Definition 1.

Definition 1 (Multi-Agent Controllability). *Given an arbitrary target state $x^k \in \mathbb{R}^{n \times 1}$ at stage $k \in \mathcal{K}$ and an initial state $x^0 \in \mathbb{R}^{n \times 1}$, the system (1) is called multi-agent controllable if and only if each player $i \in \mathcal{N}$ can find a sequence of finite control actions to reach x^k in expectation, regardless of the potential type realization $\theta \in \Theta$ and other players' action sequences $u_{-i}^{0:k}$.*

A. Forward Belief Update

At each stage $k \in \mathcal{K}$, the information available to player i consists all players' state history $h^k := \{x^0, \dots, x^k\} \in \mathcal{H}^k$ as well as his own type value θ_i . Define $\Delta(\Theta_{-i})$ as the set of probability distributions over set Θ_{-i} . Each player i at stage k forms a belief $l_i^k : \mathcal{H}^k \times \Theta_i \mapsto \Delta(\Theta_{-i})$ based on his available information. Thus, $l_i^k(\cdot|h^k, \theta_i)$ is a probability measure of other players' types; i.e., $\sum_{\bar{\theta}_{-i} \in \Theta_{-i}} l_i^k(\bar{\theta}_{-i}|h^k, \theta_i) = 1, \forall h^k \in \mathcal{H}^k, \theta_i \in \Theta_i$. The new arrival of state observation x^{k+1} leads to the following Bayesian update at stage $k+1$ for all $\theta_{-i} \in \Theta_{-i}$:

$$l_i^{k+1}(\theta_{-i}|h^{k+1}, \theta_i) = \frac{l_i^k(\theta_{-i}|h^k, \theta_i) \Pr(x^{k+1}|\theta_{-i}, x^k, \theta_i)}{\sum_{\bar{\theta}_{-i} \in \Theta_{-i}} l_i^k(\bar{\theta}_{-i}|h^k, \theta_i) \Pr(x^{k+1}|\bar{\theta}_{-i}, x^k, \theta_i)}. \quad (2)$$

In (2), we use the facts of $\Pr(h^k, \theta_i) = 1$ under the observable history h^k at stage k and the Markov state dynamics $\Pr(x^{k+1}|\theta_{-i}, h^k, \theta_i) = \Pr(x^{k+1}|\theta_{-i}, x^k, \theta_i) = d_w(x^{k+1} - f^k(x^k, u^k, \theta))$. The denominator is bigger than 0 as $w^k \in \mathbb{R}^{n \times 1}$.

B. Nonzero-Sum Cost Function and Equilibrium Concepts

At non-terminal stage $k \in \mathcal{K} \setminus \{K\}$, player i 's cost function is $g_i^k : \mathbb{R}^{n \times 1} \times \prod_{i=1}^N \mathbb{R}^{m_i \times 1} \times \Theta_i \mapsto \mathbb{R}$. The final stage cost is $g_i^K : \mathbb{R}^{n \times 1} \times \Theta_i \mapsto \mathbb{R}$. Player i 's expected cumulative cost from arbitrary initial stage $k_0 \in \mathcal{K}$ to the terminal stage K is shown in (3). The expectations are taken first over the external noise sequence w^k and then over other players' internal type uncertainty. We can only exchange the order of these two expectations if l_i^k is independent of w^{k-1} , e.g., under the level-0 Bayesian Nash equilibrium defined in Definition 4.

$$J_i^{k_0}(l_i^{k_0:K-1}, u^{k_0:K-1}, x^{k_0}, \theta_i) = \mathbb{E}_{w^{K-1} \sim d_w} [g_i^K(x^K, \theta_i)] + \sum_{k=k_0}^{K-1} \mathbb{E}_{w^{k-1} \sim d_w} \left[\mathbb{E}_{\theta_{-i} \sim l_i^k} [g_i^k(x^k, u^k, \theta_i)] \right]. \quad (3)$$

Each player i at stage $k_0 \in \mathcal{K}$ aims to minimize $J_i^{k_0}$ by choosing his action $u_i^k, \forall k \in \{k_0, \dots, K-1\}$, based on the available information h^k, θ_i , which results in the definition of sequential rationality in Definition 2. Define $u_i^{k_0:K} := \{u_i^{k_0}, \dots, u_i^K\}$ as player i 's action sequence from stage k_0 to K and $u^{k_0:K} := \{u_i^{k_0:K}, u_{-i}^{k_0:K}\}$ as player i 's and all other players' control sequences from stage k_0 to K .

Definition 2 (Sequential Rationality). *Player i 's action sequence $u_i^{*,k_0:K-1}$ is called sequentially rational under a given sequence of belief $l_i^{k_0:K-1}$ and type θ_i , if $\forall i \in \mathcal{N}, \forall k_0 \in \mathcal{K}, \forall u_i^{k_0:K-1}, x^{k_0}$,*

$$V_i^{k_0}(l_i^{k_0:K-1}, x^{k_0}, \theta_i) := J_i^{k_0}(l_i^{k_0:K-1}, u_i^{*,k_0:K-1}, u_{-i}^{*,k_0:K-1}, x^{k_0}, \theta_i) \leq J_i^{k_0}(l_i^{k_0:K-1}, u_i^{k_0:K-1}, u_{-i}^{*,k_0:K-1}, x^{k_0}, \theta_i).$$

We can use dynamic programming to obtain the following recursive form for all $k \in \mathcal{K} \setminus \{K\}$ with the boundary condition $V_i^K(x^K, \theta_i) = g_i^K(x^K, \theta_i)$; i.e.,

$$V_i^k(l_i^{k:K-1}, x^k, \theta_i) = \min_{u_i^k} \sum_{\bar{\theta}_{-i}} l_i^k(\bar{\theta}_{-i} | h^k, \theta_i) \{g_i^k(x^k, u^k, \theta_i) + \mathbb{E}_{w^k \sim d_w} [V_i^{k+1}(l_i^{k+1:K-1}, f^k(x^k, u^k, \theta_i, \bar{\theta}_{-i}) + w^k, \theta_i)]\}. \quad (4)$$

Since each player at initial stage $k_0 \in \mathcal{K}$ aims to determine the action sequence $u_i^{k_0:K-1}$ which couples with his belief sequence $l_i^{k_0:K-1}$ in the future stages, we define how players obtain their future beliefs based on different belief-consistency levels in Definition 3. A perfect belief-consistent Bayesian player considers the potential belief update for the entire $t = K - k_0$ future stages. A Bayesian player with bounded belief consistency only considers a potential belief update of $t < K - k_0$ stages and assumes that the beliefs at the remaining stages $k \in \{k_0 + t, \dots, K-1\}$ equal the up-to-date belief $l_i^{k_0+t}$.

Definition 3 (Belief Consistency). *Player i 's belief sequence $l_i^{k_0:K-1}$ is called level- t consistent with the action sequence $u^{k_0:K-1}$ if $l_i^{k_0:k_0+t}$ under $u^{k_0:K-1}$ satisfies the belief update in (2) and $l_i^k = l_i^{k_0+t}, \forall k \in \{k_0 + t, \dots, K-1\}$.*

We define the level- t Bayesian Nash Equilibrium (BNE) for N players in Definition 4 based on the requirement of sequential rationality in Definition 2 and level- t belief consistency in Definition 3.

Definition 4 (Level- t Bayesian Nash Equilibrium). *In the dynamic game of incomplete information defined by 1, 3, and 2, N players' action sequence $u^{*,k_0:K-1}$ consists the level- t BNE if $u_i^{*,k_0:K-1}$ is sequential rational under the belief sequence $l_i^{k_0:K-1}$ and $l_i^{k_0:K-1}$ is level- t consistent with $u_i^{*,k_0:K-1}$ for every $i \in \mathcal{K}$ and $k_0 \in \mathcal{K}$. If $t = K - k_0$, we further call the equilibrium as the Perfect Bayesian Nash Equilibrium (PBNE).*

Time-consistency of the equilibrium is an indicator of the robustness of the solutions subject to perturbations. Based on Definition 5.14 in [41], Lemma 1 discusses the weak and strong time consistency. The weak time-consistency states that the equilibrium action is time-consistent on the equilibrium state trajectory while the strong time-consistency further guarantees that it is time-consistent for all potential state trajectories.

Lemma 1 (Time Consistency). *The action sequence under the level- t BNE is Weakly Time-Consistent (WTC) if $t = K - k_0$, and is time-inconsistent for all $t < K - k_0$. If $l_i^{k_0}(\theta_{-i} | x^{k_0}, \theta_i) \in \{0, 1\}, \forall i \in \mathcal{N}, \forall \theta_{-i} \in \Theta_{-i}$, the action sequence is Strongly Time-Consistent (STC) for all $t \in \{0, \dots, K - k_0\}$.*

Proof. If $t < K - k_0$, then the belief of the truncation game at stage $k > k_0 + t$ is different from the resulted belief of the original game, which results in a different action profile and is time inconsistent. If $t = K - k_0$, then the belief of all truncation games will be the same if and only if all players follow the equilibrium. Thus, the action sequence under PBNE is WTC yet not STC. If the initial belief $l_i^{k_0} \in \{0, 1\}$, then future state observations do not

affect future beliefs; i.e., $l_i^k \equiv l_i^{k_0}, \forall k \in \{k_0, \dots, K\}$. Thus, all players' types are of complete information and the BNE under any $t \in \{0, \dots, K - k_0\}$ degenerates to the same Nash equilibrium of dynamic games with complete information. \square

Due to the time inconsistency of other level-t BNE, each player needs to recompute his action sequence and update the belief every t stages. Similar to the receding horizon control, players under level-t BNE at the initial stage k_0 will compute the action sequence of all the future stages yet only implement the first t -stage actions. Then, each player updates the belief and recomputes the level-t BNE at the new initial stage $k_0 + t$. They repeat the above process until reaching the final stage. We visualize PBNE and level-0 BNE in figure 1.

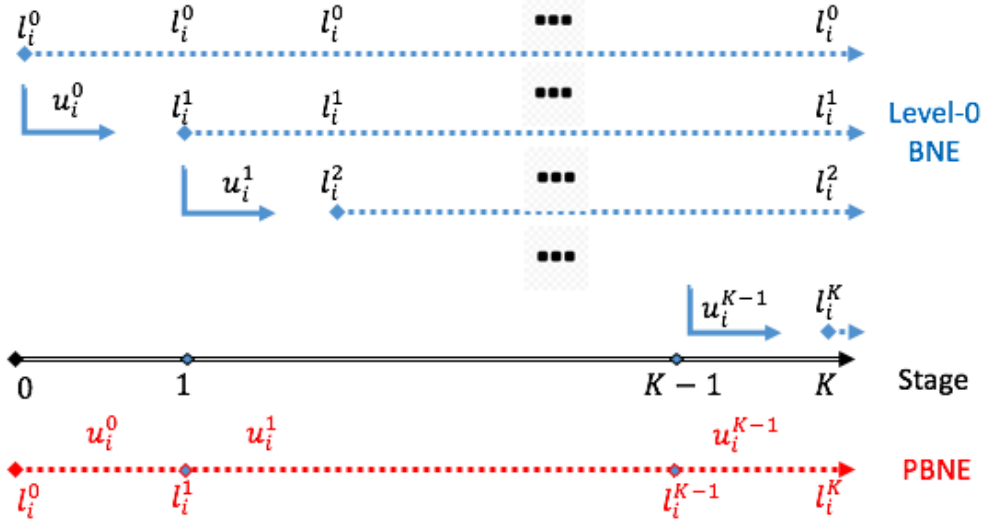


Fig. 1: An illustration of PBNE and level-0 BNE in red and blue, respectively. Players update their future-stage beliefs during the action computation phase under PBNE but do not under level-0 BNE. For all level-t BNE, players update their beliefs after reaching the future stage with observation x^k .

C. Computations of PBNE

Since players' beliefs are consistent with their actions over K stages under the PBNE, we can assimilate player i 's belief represented by the vector $\beta_i^k := [l_i^k(\theta_{-i})]_{\theta_{-i} \in \Theta_{-i}}$ into the system state at each stage k to form an expanded state $y^k := \{x^k, \beta_1^k, \dots, \beta_N^k\}, k \in \mathcal{K}$. We can obtain a Markov transition function Y^k for the expended state as $y^{k+1} = Y^k(y^k, u^k, \theta, w^k)$ by combining (1) and (2). We can further represent the objective function $J_i^{k_0}$ equivalently as $\tilde{J}_i^{k_0}(l_i^{k_0}, u^{k_0:K-1}, x^{k_0}, \theta_i) := \sum_{k=k_0}^K \mathbb{E}_{w^{k-1} \sim d_w} [\tilde{g}_i^k(y^k, u^k, \theta_i)]$, where we obtain \tilde{g}_i^k based on (3). Since the new transition function $Y^k, \forall k \in \mathcal{K}$, already guarantees the K -stage belief consistency, we only need to solve (4) to obtain the equilibrium action $u^{*,k_0:K-1}$. Define $\tilde{V}_i^{k_0}(l_i^{k_0}, x^{k_0}, \theta_i) := \tilde{J}_i^{k_0}(l_i^{k_0}, u^{*,k_0:K-1}, x^{k_0}, \theta_i)$, (4) can be represented equivalently as $\tilde{V}_i^k(y^k, \theta_i) = \min_{u_i^k} \tilde{g}_i^k(y^k, u^k, \theta_i) + \mathbb{E}_{w^{k-1} \sim d_w} [\tilde{V}_i^{k+1}(y^{k+1}, \theta_i)]$, $\forall i \in \mathcal{N}, \forall \theta_i \in \Theta_i$, which can be solved backwardly from stage $K - 1$ to 0. The $(k+1)$ -stage results of $u_i^{*,k+1}, \tilde{V}_i^{k+1}$ are applied to compute $u_i^{*,k}, \tilde{V}_i^k$ at stage k and each $u_i^{*,k}$ is a feedback of y^k . Although we can obtain the PBNE using the above recursive form, the computation is challenging without approximations or additional structures of the problem. In the following sections, we focus on the level-0 BNE for players with bounded belief consistency and the Linear-Quadratic (LQ) structures to reduce the computation complexity and further obtain explicit and practical actions. Equilibrium actions in nonlinear stochastic systems with general cost functions can be obtained by applying LQ methods iteratively [42]. Conjugate prior assumptions can be adopted to simplify the Bayesian update and obtain PBNE explicitly [43], [44].

III. LINEAR-QUADRATIC SPECIFICATION

In the following sections, we consider linear state dynamics

$$f^k(x^k, u^k, \theta) := A^k(\theta)x^k + \sum_{\bar{i}=1}^N B_{\bar{i}}^k(\theta_{\bar{i}})u_{\bar{i}}^k, \quad (5)$$

with stage-varying matrices $A^k(\theta) \in \mathbb{R}^{n \times n}$, $B_{\bar{i}}^k(\theta_{\bar{i}}) \in \mathbb{R}^{n \times m_{\bar{i}}}$. Each player i 's cost is quadratic in both x^k and u^k ; i.e.,

$$g_i^k(x^k, u^k, \theta_i) = (x^k - x_{d_i}^k(\theta_i))' D_i^k(\theta_i) (x^k - x_{d_i}^k(\theta_i)) + f_{d_i}^k(x_{d_i}^k(\theta_i)) + \sum_{j=1}^N (u_j^k)' F_{ij}^k(\theta_i) u_j^k, \forall k \in \mathcal{K}, \quad (6)$$

where $\{x_{d_i}^k(\theta_i)\}_{k \in \mathcal{K}}$ is a known type-dependent reference trajectory for player $i \in \mathcal{N}$ and $f_{d_i}^k$ is a known function of $x_{d_i}^k(\theta_i)$. The cost matrices $D_i^k(\theta_i) \in \mathbb{R}^{n \times n}$, $F_{ij}^k(\theta_i) \in \mathbb{R}^{m_i \times m_j}$, $\forall i, j \in \mathcal{N}, k \in \mathcal{K}$, are symmetric and do not need to be positive definite as shown in Section IV. At the final stage, $F_{ij}^K(\theta_i) \equiv \mathbf{0}_{m_i m_j}$, $\forall i, j \in \mathcal{N}, \forall \theta_i \in \Theta_i$. Under the linear-quadratic specification, we obtain the necessary and sufficient condition for multi-agent controllability in Lemma 2 and the closed form of state-feedback action $u_i^{*,k}$ and the value function V_i^k at the equilibrium in Theorem 1.

Lemma 2. *System (5) is multi-agent controllable if and only if matrix*

$$H_i^k(\theta) := [B_i^{k-1}(\theta_i), \dots, \prod_{\bar{k}=2}^{k-1} A^{\bar{k}}(\theta) B_i^1(\theta_i), \prod_{\bar{k}=1}^{k-1} A^{\bar{k}}(\theta) B_i^0(\theta_i)], \forall i \in \mathcal{N}, \forall \theta \in \Theta, \forall k \in \mathcal{K},$$

is of full rank.

Proof. Since the noise sequence w^k is of zero mean, we obtain $\mathbb{E}[x^k] = \prod_{\bar{k}=0}^{k-1} A^{\bar{k}} x^0 + \sum_{\bar{i}=1}^N H_{\bar{i}}^k(\theta) [u_{\bar{i}}^{k-1}; \dots; u_{\bar{i}}^0], \forall k \in \mathcal{K}$, by induction. Thus, $H_i^k(\theta)$ is required to be of full rank. \square

Notations for Theorem 1: Let a sequence of symmetric matrices $S_i^k(l_i^k, \theta_i) \in \mathbb{R}^{n \times n}$, vectors $N_i^k(l_i^k, \theta_i) \in \mathbb{R}^{n \times 1}$, and scalars $q_i^k(l_i^k, \theta_i) \in \mathbb{R}$ satisfy the set of extended Riccati equations in (7),(8),(9) for all $i \in \mathcal{N}, k \in \{0, \dots, K-1\}, \theta_i \in \Theta_i, l_i^k$. Let matrix $\mathbf{M}_i^k(\theta_i^l) \in \mathbb{R}^{m_i \times \sum_{\bar{i}=1}^N m_{\bar{i}} N_{\bar{i}}}, l \in \{1, 2, \dots, N_i\}, i \in \mathcal{N}, k \in \{0, \dots, K-1\}$, be the truncated row block, i.e., from row $\sum_{\bar{i}=1}^{i-1} m_{\bar{i}} N_{\bar{i}} + m_i(l-1)$ to $\sum_{\bar{i}=1}^{i-1} m_{\bar{i}} N_{\bar{i}} + m_i l$, of matrix $(-\mathbf{W}^{0,k})^{-1}$, where matrices $\mathbf{W}^{0,k}, \mathbf{W}^{1,k}, \mathbf{W}^{2,k}$ are defined in (11).

$$\begin{aligned} S_i^k &= D_i^k + \mathbb{E}_{\theta_{-i} \sim l_i^k} \left[(A^k(\theta) + \sum_{j=1}^N B_j^k(\theta_j) \mathbf{M}_j^k(\theta_j) \mathbf{W}^{1,k})' S_i^{k+1} (A^k(\theta) + \sum_{j=1}^N B_j^k(\theta_j) \mathbf{M}_j^k(\theta_j) \mathbf{W}^{1,k}) + \right. \\ &\quad \left. \sum_{j=1}^N (\mathbf{M}_j^k(\theta_j) \mathbf{W}^{1,k})' F_{ij}^k \mathbf{M}_j^k(\theta_j) \mathbf{W}^{1,k} \right]; S_i^K = D_i^K. \end{aligned} \quad (7)$$

$$\begin{aligned} N_i^k &= -2D_i^k x_{d_i}^k + \mathbb{E}_{\theta_{-i} \sim l_i^k} \left[(\sum_{j=1}^N B_j^k(\theta_j) \mathbf{M}_j^k(\theta_j) \mathbf{W}^{1,k} + A^k(\theta))' (N_i^{k+1} + 2S_i^{k+1} \sum_{j=1}^N B_j^k(\theta_j) \mathbf{M}_j^k(\theta_j) \mathbf{W}^{2,k}) + \right. \\ &\quad \left. 2 \sum_{j=1}^N (\mathbf{M}_j^k(\theta_j) \mathbf{W}^{1,k})' F_{ij}^k \mathbf{M}_j^k(\theta_j) \mathbf{W}^{2,k} \right]; N_i^K = -2D_i^K x_{d_i}^K. \end{aligned} \quad (8)$$

$$\begin{aligned} q_i^k &= \text{Tr}(S_i^{k+1} Q^k) + q_i^{k+1} + (x_{d_i}^k)' D_i^k(x_{d_i}^k) + f_{d_i}^k(x_{d_i}^k) \mathbb{E}_{\theta_{-i} \sim l_i^k} \left[(\sum_{j=1}^N B_j^k(\theta_j) \mathbf{M}_j^k(\theta_j) \mathbf{W}^{2,k})' N_i^{k+1} + \right. \\ &\quad \left. (\sum_{j=1}^N B_j^k(\theta_j) \mathbf{M}_j^k(\theta_j) \mathbf{W}^{2,k})' S_i^{k+1} (\sum_{j=1}^N B_j^k(\theta_j) \mathbf{M}_j^k(\theta_j) \mathbf{W}^{2,k}) + \sum_{j=1}^N (\mathbf{M}_j^k(\theta_j) \mathbf{W}^{2,k})' F_{ij}^k \mathbf{M}_j^k(\theta_j) \mathbf{W}^{2,k} \right]; \\ q_i^K &= (x_{d_i}^K)' D_i^K x_{d_i}^K + f_{d_i}^K(x_{d_i}^K). \end{aligned} \quad (9)$$

Define a sequence of m_i -by- m_i square matrices $R_i^k(l_i^k, \theta_i) := F_{ii}^k(\theta_i) + (B_i^k(\theta_i))' S_i^{k+1}(l_i^k, \theta_i) B_i^k(\theta_i)$, $(\sum_{\bar{i}=1}^N N_{\bar{i}} n_{\bar{i}})$ -by- $(N_i m_i)$ block matrices $\mathbf{B}_i^k := \text{Diag}[B_i^k(\theta_i^1) \dots, B_i^k(\theta_i^{N_i})]$, $(\sum_{\bar{i}=1}^N N_{\bar{i}} m_{\bar{i}})$ -by- $(\sum_{\bar{i}=1}^N N_{\bar{i}} m_{\bar{i}})$ block matrices $\mathbf{S}_i^k := \text{Diag}[S_i^k(l_i^k, \theta_i^1)]$,

, $\dots, S_i^k(l_i^k, \theta_i^{N_i})]$ for all $i \in \mathcal{N}, l_i^k, \theta_i \in \Theta_i, k \in \{0, \dots, K-1\}$. Define the belief matrix for all $i, j \in \mathcal{N}, j \neq i, k \in \{0, \dots, K-1\}$:

$$\mathbf{L}_{ij}^k := \begin{bmatrix} \mathbf{L}_i^k(\theta_j^1|h^k, \theta_i^1), & \dots & \mathbf{L}_i^k(\theta_j^{N_j}|h^k, \theta_i^1) \\ \mathbf{L}_i^k(\theta_j^1|x^k, \theta_i^2), & \dots & \mathbf{L}_i^k(\theta_j^{N_j}|h^k, \theta_i^2) \\ \vdots & \ddots & \vdots \\ \mathbf{L}_i^k(\theta_j^1|h^k, \theta_i^{N_i}), & \dots & \mathbf{L}_i^k(\theta_j^{N_j}|h^k, \theta_i^{N_i}) \end{bmatrix}, \quad (10)$$

where each block element $\mathbf{L}_i^k(\theta_j^1|h^k, \theta_i^1) = \text{Diag}[l_i^k(\theta_j^1|h^k, \theta_i^1), \dots, l_i^k(\theta_j^1|h^k, \theta_i^1)] \in \mathbb{R}^{n \times n}$. Since all its elements are positive and all rows sum to one, the belief matrix \mathbf{L}_{ij}^k is a *right stochastic matrix*. Furthermore, define parameter matrices $\mathbf{W}^{1,k} = [W_1^{1,k}; \dots; W_N^{1,k}] \in \mathbb{R}^{\sum_{i=1}^N m_i N_i \times n}$, $\mathbf{W}^{2,k} = [W_1^{2,k}; \dots; W_N^{2,k}] \in \mathbb{R}^{\sum_{i=1}^N m_i N_i \times 1}$, and $\mathbf{W}^{0,k} := [W_{ij}^{0,k} \in \mathbb{R}^{m_i N_i \times m_j N_j}]_{i,j \in \mathcal{N}}$, whose elements are given as follows:

$$\begin{aligned} W_i^{1,k} &:= \left[(B_i^k(\theta_i^1))' S_i^{k+1}(l_i^k, \theta_i^1) \mathbb{E}_{\theta_{-i} \sim l_i^k} [A^k(\theta_i^1, \theta_{-i})]; \dots; (B_i^k(\theta_i^{N_i}))' S_i^{k+1}(l_i^k, \theta_i^{N_i}) \mathbb{E}_{\theta_{-i} \sim l_i^k} [A^k(\theta_i^{N_i}, \theta_{-i})] \right], \\ W_i^{2,k} &:= \frac{1}{2} \left[(B_i^k(\theta_i^1))' N_i^{k+1}(l_i^k, \theta_i^1); \dots; (B_i^k(\theta_i^{N_i}))' N_i^{k+1}(l_i^k, \theta_i^{N_i}) \right], \\ W_{ii}^{0,k} &= \text{Diag}[R_i^k(l_i^k, \theta_i^1), \dots, R_i^k(l_i^k, \theta_i^{N_i})], \\ W_{ij}^{0,k} &= (\mathbf{B}_i^k)' \mathbf{S}_i^{k+1} \mathbf{L}_{ij}^k \mathbf{B}_j^k, \forall j \in \mathcal{N} \setminus \{i\}. \end{aligned} \quad (11)$$

Players' types affect their actions. With a little abuse of notation, we write the action as a function of θ_i ; i.e., $u_i^k = u_i^k(\theta_i)$ and define the action vectors $\mathbf{u}_i^k := [u_i^k(\theta_i^1), \dots, u_i^k(\theta_i^{N_i})]' \in \mathbb{R}^{m_i N_i \times 1}$, $\mathbf{u}^k := [\mathbf{u}_1^k, \mathbf{u}_2^k \dots, \mathbf{u}_N^k]' \in \mathbb{R}^{\sum_{i=1}^N m_i N_i \times 1}$.

Theorem 1. *The LQ game of incomplete information defined by 5, 6, and 2 admits a unique state-feedback level-0 BNE*

$$u_i^{*,k}(l_i^k, x^k, \theta_i) = \mathbf{M}_i^k(\theta_i) \mathbf{W}^{1,k} x^k + \mathbf{M}_i^k(\theta_i) \mathbf{W}^{2,k}, \forall i, k, \quad (12)$$

if and only if $R_i^k(l_i^k, \theta_i)$ is positive definite and $\mathbf{W}^{0,k}$ is non-singular for all $i \in \mathcal{N}, \theta_i \in \Theta_i, k \in \{0, \dots, K-1\}, l_i^k$. The corresponding value function V_i^k at each stage depends only on the current-stage belief l_i^k and is quadratic in x^k ; i.e.,

$$V_i^k(l_i^{k:K-1}, x^k, \theta_i) = q_i^k(l_i^k, \theta_i) + (x^k)' N_i^k(l_i^k, \theta_i) + (x^k)' S_i^k(l_i^k, \theta_i) x^k, \forall i \in \mathcal{N}, k \in \mathcal{K}. \quad (13)$$

Proof. We use induction to prove the result. At the final stage K , the value function

$$V_i^K(l_i^K, \theta_i) = (x^K - x_{d_i}^K(\theta_i))' D_i^K(\theta_i) (x^K - x_{d_i}^K(\theta_i)) + f_{d_i}^K(x_{d_i}^K(\theta_i))$$

is quadratic in x^K and we obtain the boundary conditions for S_i^K, N_i^K, q_i^K in (7),(8),(9), respectively. At any stage $k \in \{0, \dots, K-1\}$, suppose (13) is true at stage $k+1$, i.e., V_i^{K+1} is quadratic in $x^{k+1} = A^k(\theta) x^k + \sum_{i=1}^N B_i^k(\theta_i) u_i^k$, the right-hand side of (4) is quadratic in u_i^k for each player i as $R_i^k(l_i^k, \theta_i)$ is positive definite. Then, the first-order necessary conditions for minimization are also sufficient and we obtain the following unique set of equations by differentiation:

$$-R_i^k u_i^{*,k} = (B_i^k)' S_i^{k+1} \mathbb{E}_{\theta_{-i} \sim l_i^k} [A^k] x^k + \frac{1}{2} (B_i^k)' N_i^{k+1} + (B_i^k)' S_i^{k+1} \sum_{j \neq i} \mathbb{E}_{\theta_j \sim l_i^k} [B_j^k(\theta_j) u_j^{*,k}(\theta_j)]. \quad (14)$$

Equation (14) can be written in the matrix form given the existence of $(-\mathbf{W}^{0,k})^{-1}$; i.e.,

$$\mathbf{u}^{*,k} = (-\mathbf{W}^{0,k})^{-1} (\mathbf{W}^{1,k} x^k + \mathbf{W}^{2,k}), \quad (15)$$

which results in the equilibrium action $u_i^{*,k}$ in (12). Finally, substitute the equilibrium action $u_i^{*,k}$ into the right-hand side of (4). Since $l_i^k = l_i^{k+1}$ for the level-0 BNE and $\mathbb{E}_{w^k \sim d_w} [(w^k)' S_i^{k+1} w^k] = \text{Tr}(S_i^{k+1} Q^k)$, the value function $V_i^k(l_i^k, \theta_i)$ at stage k can also be represented in the same form of (13) where S_i^k, N_i^k, q_i^k satisfy (7),(8),(9), respectively. \square

We can obtain an alternative form of S_i^k by getting rid of player i 's self-dependency as shown in Corollary 1. The alternative forms of N_i^k and q_i^k can also be obtained based on the same method given in the proof. Define $G_i^k(l_i^k, \theta_i) := \mathbf{I}_n - B_i^k(\theta_i) (R_1^k(l_i^k, \theta_i))^{-1} (B_i^k(\theta_i))' S_i^{k+1}(l_i^k, \theta_i)$.

Corollary 1 (Alternative Extended Riccati Equations). *Equation (7) is equivalent to $S_i^K = D_i^K; S_i^k = D_i^k + \mathbb{E}_{\theta_{-i} \sim l_i^k} [(A + \sum_{j \neq i} B_j^k(\theta_j) \mathbf{M}_j^k(\theta_j) \mathbf{W}^{1,k})' (G_i^k)' S_i^{k+1} (A + \sum_{j \neq i} B_j^k(\theta_j) \mathbf{M}_j^k(\theta_j) \mathbf{W}^{1,k}) + \sum_{j \neq i} (\mathbf{M}_j^k(\theta_j) \mathbf{W}^{1,k})' F_{ij}^k \mathbf{M}_j^k(\theta_j) \mathbf{W}^{1,k}]$.*

Proof. Based on (12) and (14), $-R_i^k \mathbf{M}_i^k(\theta_i) \mathbf{W}^{1,k} = (B_i^k)' S_i^{k+1} \mathbb{E}_{\theta_{-i} \sim l_i^k} [A^k + \sum_{j \neq i} B_j^k(\theta_j) \mathbf{M}_j^k(\theta_j) \mathbf{W}^{1,k}]$ and $-R_i^k \mathbf{M}_i^k(\theta_i) \mathbf{W}^{2,k} = \mathbb{E}_{\theta_{-i} \sim l_i^k} [(B_i^k)' S_i^{k+1} \sum_{j \neq i} B_j^k(\theta_j) \mathbf{M}_j^k(\theta_j) \mathbf{W}^{2,k}] + \frac{1}{2} (B_i^k)' N_i^{k+1}$. Then, we can show that $A^k + \sum_{j=1}^N B_j^k(\theta_j) \mathbf{M}_j^k(\theta_j) \mathbf{W}^{1,k} = G_i^k (A^k + \sum_{j \neq i} B_j^k(\theta_j) \mathbf{M}_j^k(\theta_j) \mathbf{W}^{1,k})$ and $(G_i^k)' S_i^{k+1} G_i^k + S_i^{k+1} B_i^k (R_i^k)^{-1} F_{ii}^k (R_i^k)^{-1} (B_i^k)' S_i^{k+1} = (G_i^k)' S_i^{k+1}$, which results in the equation in Corollary 1. \square

Besides the coupling between the state dynamics and the cost structure, the type uncertainty in our game also results in a coupling of players' beliefs. The right stochastic matrix in (10) indicates the belief coupling. Therefore, each player i 's actions are not only affected by the parameters of state dynamics, i.e., $A^k, B_i^k, \bar{i} \in \mathcal{N}$, and all players' cost parameters $D_i^k, F_{ij}^k, \bar{i}, \bar{j} \in \mathcal{N}$, but also all players' beliefs $l_i^k, \bar{i} \in \mathcal{N}$. Thus, player i can change other players' actions if he can manipulate their beliefs of his type θ_i , i.e., $l_j^k, \forall j \in \mathcal{N} \setminus \{i\}$, or make them believe that his belief l_i^k on their types θ_{-i} have changed.

Since the above three couplings may not coexist, we provide three decoupling structures in Definition 5, 6, and 7 with the following notations. For each type $\theta_i \in \Theta_i$, we divide $A^k(\theta), D_i^k(\theta_i), S_i^k(\theta_i)$ into N -by- N blocks where the (i, i) block is $A_i^k(\theta), \bar{D}_i^k(\theta_i), \bar{S}_i^k(\theta_i) \in \mathbb{R}^{n_i \times n_i}$, respectively. The i -th, $i \in \mathcal{N}$, row block of $N_i^k(\theta_i), x_{d_i}^k(\theta_i)$ is $\bar{N}_i^k(\theta_i), \bar{x}_{d_i}^k(\theta_i) \in \mathbb{R}^{n_i \times 1}$, respectively. The i -th, $i \in \mathcal{N}$, row block of $B_i^k(\theta_i)$ is $\bar{B}_i^k(\theta_i) \in \mathbb{R}^{n_i \times m_i}$.

Definition 5 (Decoupled Dynamics). *Player i has decoupled dynamics if for all $k \in \mathcal{K}$, $A_i^k(\theta) = \bar{A}_i^k(\theta_i), \forall \theta \in \Theta$, while all other elements in the i -th row block and the i -th column block of $A^k(\theta)$ are 0. Besides, all elements of $B_i^k(\theta_i)$ except for the row block $\bar{B}_i^k(\theta_i)$ are required to be 0.*

Definition 6 (Decoupled Cost). *Player i has a decoupled cost if for all stage $k \in \mathcal{K}$, $F_{ij}^k(\theta_i) = \mathbf{0}_{m_i, m_i}, \forall \theta_i \in \Theta_i, i, j \in \mathcal{N}, j \neq i$, and all elements of $D_i^k(\theta_i)$ equal 0 except for $\bar{D}_i^k(\theta_i), \forall i \in \mathcal{N}$.*

Definition 7 (Decoupled Cognition). *Player i has decoupled cognition if all N players' beliefs do not affect his actions throughout K stages.*

The decoupled state dynamics and decoupled cost structure of player i together result in the decoupled cognition as shown in Corollary 2. In this case, player i only needs to solve a LQ optimal control problem to determine his optimal action sequence which is not affected by other players' actions. If each player only has one type, i.e., $N_i = 1, \forall i \in \mathcal{N}$, or all players' beliefs are *common knowlege* throughout K stages, e.g., the initial belief $l_i^0 \in \{0, 1\}, \forall i \in \mathcal{N}$, then each player has the decoupled cognition structure and the proposed game degenerates to the classical N -person LQ game [41]. We omit θ_i when there is no ambiguity.

Corollary 2 (Degeneration to LQ Control). *If player i has both the decoupled state dynamics and a decoupled cost, then he has a decoupled cognition structure and his action under any level- t BNE is independent of other players' actions; i.e., $u_i^{*,k} = -(R_i^k)^{-1} (\bar{B}_i^k)' \bar{S}_i^{k+1} A_i^k x_i^k - \frac{1}{2} (R_i^k)^{-1} (\bar{B}_i^k)' \bar{N}_i^{k+1}$, where $R_i^k = F_{ii}^k + (\bar{B}_i^k)' \bar{S}_i^{k+1} \bar{B}_i^k$, $(G_i^k)' = \mathbf{I}_n - \bar{S}_i^{k+1} \bar{B}_i^k (R_i^k)^{-1} (\bar{B}_i^k)'$, $\bar{S}_i^k = (A_i^k)' (G_i^k)' \bar{S}_i^{k+1} A_i^k + \bar{D}_i^k$, and $\bar{N}_i^k = (A_i^k)' (G_i^k)' \bar{N}_i^{k+1} - 2 \bar{D}_i^k \bar{x}_{d_i}^k$.*

Proof. We show by induction that $S_i^k, N_i^k, \forall k \in \mathcal{K}$, satisfy the following sparse condition: only the (i, i) block of S_i^k and the i -th row block of N_i^k are nonzero. At stage K , $S_i^K = D_i^K$ and $N_i^K = -2 D_i^K x_{d_i}^K$ satisfy the above sparse condition. At stage $k \in \{0, \dots, K-1\}$, if S_i^{k+1}, N_i^{k+1} satisfy the sparse condition, $\mathbf{W}^{0,k}$ becomes a diagonal block matrix where $W_{ij}^{0,k} = \mathbf{0}_{m_i N_i, m_j N_j}$ and $\mathbf{M}_i^k(\theta_i) = -(R_i^k(\theta_i))^{-1}$. Then S_i^k, N_i^k have the same forms as S_i^{k+1}, N_i^{k+1} based on (7) and (8) and we obtain the new recursive forms of \bar{S}_i^k, \bar{N}_i^k and $u_i^{*,k}$ in Corollary 2. \square

Due to the time inconsistency of the level-0 BNE, players need to recompute the equilibrium actions with the updated beliefs when observing new state x^{k+1} at every stage. We summarize the computation and implementation procedure under the LQ specification in Algorithm 1 where k is the real-time stage index. At each stage k , each player i with belief l_i^k first computes $S_i^{k_0}(l_i^{k_0}, \theta_i), \forall \theta_i \in \Theta_i$, in (7) backwardly from stage $k_0 = K-1$ to $k_0 = k$ under the assumption that all players do not consider the updated beliefs during the computation phase. Next, player i computes $N_i^{k_0}(l_i^{k_0}, \theta_i), \forall \theta_i \in \Theta_i$, in (8) backwardly from stage $k_0 = K-1$ to $k_0 = k$ based on $S_i^{k_0+1}$ and $N_i^{k_0+1}$. Then, each player can determine the equilibrium action $\mathbf{u}^{*,k}$ at the current stage k via (15). After players apply their

actions $u_i^{*,k}, \forall i \in \mathcal{N}$, they reach stage $k+1$ with new state observation x^{k+1} , obtain the real-time cumulative cost \bar{V}_i^{k+1} , update their beliefs to l_i^{k+1} via (2), and recompute $S_i^{k_0}$ and $N_i^{k_0}$ backwardly from $k_0 = K-1$ to $k_0 = k+1$ to determine the new control action u_i^{k+1} . They repeat the above procedures until reaching the terminal stage $k = K$.

Algorithm 1: Implementation of Level-0 BNE

```

1 Initialize  $k = 0$ ,  $\bar{V}_i^0(\theta_i) = 0$ , and  $l_i^0, \forall i \in \mathcal{N}, \forall \theta_i \in \Theta_i$ ;
2 while  $k \neq K$  do
3   for  $k_0 \leftarrow K-1$  to  $k$  do
4     for  $i \leftarrow 1$  to  $N$  and  $\theta_i \leftarrow \theta_i^1$  to  $\theta_i^{N_i}$  do
5       | Compute  $S_i^{k_0}, N_i^{k_0}, q_i^{k_0}$  via (7), (8), (9) in sequence with  $l_i^{k_0} = l_i^k$ ;
6       | end
7       | Compute equilibrium actions  $\mathbf{u}^{*,k_0}$  via (15);
8     | end
9     | for  $i \leftarrow 1$  to  $N$  with  $\theta_i \in \Theta_i$  do
10    |   | Compute the real-time cumulative cost  $\bar{V}_i^{k+1}(\theta_i) = \bar{V}_i^k(\theta_i) + g_i^k(x^k, u^k, \theta_i)$ ;
11    |   | Implement action  $u_i^{*,k}$ ;
12    |   | Observe state  $x^{k+1}$  and update belief via (2);
13    |   | end
14    | Stage index update  $k \leftarrow k+1$ ;
15 end
16 Output the system state trajectory  $\{x^k\}_{k \in \mathcal{K}}$ , belief sequence  $l_i^{0:K}$ , and cumulative cost  $\{\bar{V}_i^k(\theta_i)\}_{k \in \mathcal{K}}$ 

```

A. Deceivability and Price of Deception

Effective deception can prevent or delay other players from learning the deceiver's private type. We define the criterion of successful learning of the deceiver's type in Definition 8 and ε -deceivability and ε -learnability in Definition 9.

Definition 8 (Stage of Truth Revelation). Consider player $i, j \in \mathcal{N}$ with type θ_i and θ_j , respectively. Player i 's truth-revealing stage $k_{i,j}^{tr} \in \mathcal{K} \cup \{K+1\}$ with accuracy δ satisfies two requirements. First, player i 's belief mismatch remains less than a given threshold $\delta \in (0, 1]$ after stage $k_{i,j}^{tr} \in \mathcal{K}$,

$$1 - l_i^k(\theta_j | x^k, \theta_i) \leq \delta, \forall k \geq k_{i,j}^{tr}. \quad (16)$$

Second, $k_{i,j}^{tr}$ is the first stage satisfying (16); i.e., $1 - l_i^{k_{i,j}^{tr}-1}(\theta_j | x^{k_{i,j}^{tr}-1}, \theta_i) > \delta, k_{i,j}^{tr} > 1$. If no $k_{i,j}^{tr} \in \mathcal{K}$ satisfies (16), we define $k_{i,j}^{tr} := K+1$. If there are only two players $N = 2$, we write $k_{i,j}^{tr}$ as k_i^{tr} without ambiguity.

We require $\delta \neq 0$ as the belief mismatch will not reduce to 0 in finite stage with initial belief $l_i^0 \in (0, 1)$. Due to deceivers' deceptive actions and the external noises, the belief sequence may be fluctuant; i.e., there can exist $k < k_{i,j}^{tr}$ such that $1 - l_i^k(\theta_j | x^k, \theta_i) \leq \delta$. Thus, a player should only claim a successful learning of other players' types if his belief mismatch remains less than the threshold δ for the rest of stages.

Definition 9 (Deceivability and Learnability). Consider player $i, j \in \mathcal{N}$ with type θ_i and θ_j , thresholds $\delta \in (0, 1], \varepsilon \in [0, 1]$, and a given stage index $\tilde{k} \in \mathcal{K} \cup \{K+1\}$. Player i is \tilde{k} -stage ε -deceivable if $\Pr(k_{i,j}^{tr} < \tilde{k}) \equiv \Pr(l_i^{\tilde{k}}(\theta_j | x^{\tilde{k}}, \theta_i) > 1 - \delta) \leq \varepsilon, \forall l_i^0 \in (0, 1)$. If the above does not hold, player j 's type is said to be \tilde{k} -stage ε -learnable by player i .

Since robot deception involves only a finite number of stages, it is essential that the deceived robot can learn the deceiver's type as quickly as possible so that he has sufficient stages to plan on and mitigate the deception impact from the previous stages. Therefore, the definition of learnability, i.e., non-deceivability in Definition 9 not only requires the deceived player to be capable of learning the deceiver's private information, but also learning it in a desirable rate, i.e., within \tilde{k} stage. Due to the external noise, $k_{i,j}^{tr}$ is a random variable. Thus, the definition of

learnability requires $\Pr(k_{i,j}^{tr} < \tilde{k}) > \varepsilon$; i.e., player i has a large probability to correctly learn the type of player j before stage \tilde{k} .

Definition 10 (Price of Deception). Consider the dynamic game of incomplete information defined by 1, 3, and 2 and the level-0 BNE solution concept. For the given set of parameters $\eta_0 > 0$, $\eta_i \in [0, 1], \forall i \in \mathcal{N}, \sum_{i \in \mathcal{N}} \eta_i = 1$, we define the Price of Deception (PoD) of the game as

$$p_d = \frac{\sum_{i \in \mathcal{N}} \eta_i \hat{V}_i^K(\theta_i) + \eta_0}{\sum_{i \in \mathcal{N}} \eta_i \bar{V}_i^K(\theta_i) + \eta_0} \in [0, \infty). \quad (17)$$

Motivated by the Price of Anarchy (PoA), we define the Price of Deception (PoD) in Definition 10 where $\hat{V}_i^K(\theta_i)$ represents player i 's expected cumulative cost when all players' types are *common knowledge*. The PoD is a crucial evaluation and design metric. For example, in cooperative control scenarios where robots belong to different designers, an designer may aim to minimize the total cost of their robots under deception. After the designer has chosen the weighting parameters $\eta_i, i \in \mathcal{N} \cup \{0\}$, a large p_d indicates a better accomplishment of the above goal. Unlike the PoA where selfishness leads to degraded efficiency, individual deception may increase the system utility; i.e., $p_d > 1$. Due to the external noise and the time inconsistency of the level-0 BNE, the value of \bar{V}_i^K is stochastic, which makes p_d a random variable. However, as we will see in the case study, p_d 's variance remains negligible even when \bar{V}_i^K has a large variance.

IV. DYNAMIC TARGET PROTECTION UNDER DECEPTION

We investigate the pursuit-evasion scenario in the introduction which contains $N = 2$ UAVs with the decoupled state dynamics defined in Definition 5. We omit the superscript k for time-invariant $A^k(\theta) = \mathbf{I}_4$ and $\tilde{B}_i^k(\theta_i) = [\tilde{B}_i(\theta_i), 0; 0, \tilde{B}_i(\theta_i)] \in \mathbb{R}^{2 \times 2}$ which satisfy the multi-agent controllability defined in Definition 1. We use 'she' for UAV 1, the evader and 'he' for UAV 2, the pursuer. UAV i 's state $x_i^k := [x_{i,x}^k, x_{i,y}^k]' \in \mathbb{R}^{2 \times 1}$ represents i 's location $(x_{i,x}^k, x_{i,y}^k)$ in the 2D space, and action $u_i^k = [u_{i,x}^k, u_{i,y}^k] \in \mathbb{R}^{2 \times 1}$ affects i 's speed in x and y directions.

UAV 2 as the evader selects either the harbor in 'Normandy' or 'Calais' as his final location to transmit intelligence based on his type $\theta_2 \in \{\theta_2^g, \theta_2^b\}$. He aims to reach 'Normandy' located at $\gamma(\theta_2^g) := (x^g, y^g)$ in $K = 40$ stages if his type is θ_2^g , otherwise 'Calais' located at $\gamma(\theta_2^b) := (x^b, y^b)$ if his type is θ_2^b . UAV 1 as the pursuer can make interfering signals and aims to be close to UAV 2 at the final stage to protect the harbor targeted by the evader; i.e., $g_1^k(x^k, u^k, \theta_1) = d_{12}^k(\theta_1)((x_{2,y}^k - x_{1,y}^k)^2 + (x_{2,x}^k - x_{1,x}^k)^2) + f_{11}^k(\theta_1)((u_{1,x}^k)^2 + (u_{1,y}^k)^2) - f_{12}^k(\theta_1)((u_{2,x}^k)^2 + (u_{2,y}^k)^2), \forall k \in \mathcal{K}$, where $d_{12}^k(\theta_1) = 0, \forall k \in \mathcal{K} \setminus \{K\}$. Since UAV 1 does not know the evader's type, her cost function g_1^k contains neither harbors' locations. UAV 1 is also classified into two types, i.e., $\Theta_1 = \{\theta_1^H, \theta_1^L\}$, based on her maneuverability represented by the value of $\tilde{B}_1(\theta_1)$. Given higher maneuverability $\tilde{B}_1(\theta_1^H) > \tilde{B}_1(\theta_1^L)$, the pursuer of type θ_1^H can obtain a higher speed under the same action u_1^k and thus cover a longer distance. UAV 2 also does not know the pursuer's type.

We study the deception scenario where the game model is publicly known after players' private types are revealed. Since the pursuer can learn the evader's type based on the real-time observations of state x_2^k , UAV 2 attempts to make his target ε_0 -ambiguous at all previous stages, i.e., $|d_{2,b}^k(\theta_2)/d_{2,g}^k(\theta_2) - 1| \leq \varepsilon_0, \forall \theta_2, \forall k \neq K$, and reveal his true target only at the final stage, i.e., $d_{2,g}^K(\theta_2^b) = 0, d_{2,b}^K(\theta_2^b) \gg d_{2,b}^k(\theta_2^b), \forall k \neq K$, and $d_{2,b}^K(\theta_2^g) = 0, d_{2,g}^K(\theta_2^g) \gg d_{2,g}^k(\theta_2^g) = 0, \forall k \neq K$. The evader chooses a small $\varepsilon_0 \geq 0$ and achieves the maximum ambiguity when $\varepsilon_0 = 0$. The blue lines in Fig. 2a illustrate how the evader manages to remain ambiguous in a cost-effective manner under different initial locations. Instead of remaining an equal distance to both potential targets, the evader heads toward the midpoint $((x^g + x^b)/2, (y^g + y^b)/2)$ at the early stages to confuse the pursuer.

In this case study, we suppose that the evader's true target is Calais and call θ_2^b as his *true type* and θ_2^g as the *misleading type*. We define the ratios $d_{2,g}^k(\theta_2^b)/d_{2,b}^k(\theta_2^b)$ and $d_{2,b}^k(\theta_2^g)/d_{2,g}^k(\theta_2^g)$ as the level of *trajectory deception* for the evader of type θ_2^b and θ_2^g , respectively. As shown in Fig. 2a, regardless of different initial locations, the evader who adopts a higher level of *trajectory deception* heads more toward the misleading target at the early stages. The parameters $d_{2,g}^K(\theta_2^g)$ and $d_{2,b}^K(\theta_2^b)$ represent the level of *target-reaching determination* for the evader of type θ_2^b and θ_2^g , respectively. Thus, the ratio $d_{2,b}^k(\theta_2^b)/d_{2,g}^k(\theta_2^b), \forall k \neq K$, reflects the evader's tradeoff between applying deception along the trajectory and staying close to the true target at the final stage. Fig. 2b shows that as the evader aims to deceive, his trajectory remains ambiguous for longer stages while his final location is farther away from the true target.

Besides the main goal of deceptive target reaching, UAV 2's secondary goal is to keep a distance from the pursuer along the trajectory to avoid interference; i.e., $0 \leq d_{21}^k(\theta_2^g) \ll d_{2,g}^k(\theta_2^g), 0 \leq d_{21}^k(\theta_2^b) \ll d_{2,b}^k(\theta_2^b), \forall k \in \mathcal{K}$. These two goals result in the following cost structure $g_2^k(x^k, u^k, \theta_2) = d_{2,b}^k(\theta_2)((x_{2,y}^k - y^b)^2 + (x_{2,x}^k - x^b)^2) + d_{2,g}^k(\theta_2)((x_{2,y}^k - y^g)^2 + (x_{2,x}^k - x^g)^2) + f_{22}^k(\theta_2)((u_{2,x}^k)^2 + (u_{2,y}^k)^2) - d_{21}^k(\theta_2)((x_{1,y}^k - x_{2,y}^k)^2 + (x_{1,x}^k - x_{2,x}^k)^2) - f_{21}^k(\theta_2)((u_{1,x}^k)^2 + (u_{1,y}^k)^2), \forall k \in \mathcal{K}$. The parameter $d_{21}^k(\theta_2)$ represents the level of *evasion determination* for the evader of type θ_2 at stage k . Thus, the ratio $d_{21}^k(\theta_2)/d_{2,b}^k(\theta_2)$ reflects the tradeoff between evasion and target-reaching. As the evader focuses more on keeping a distance from the pursuer along the trajectory, he takes a bigger detour and stays farther away from his true target at the final stage, which is shown in Fig. 2c.

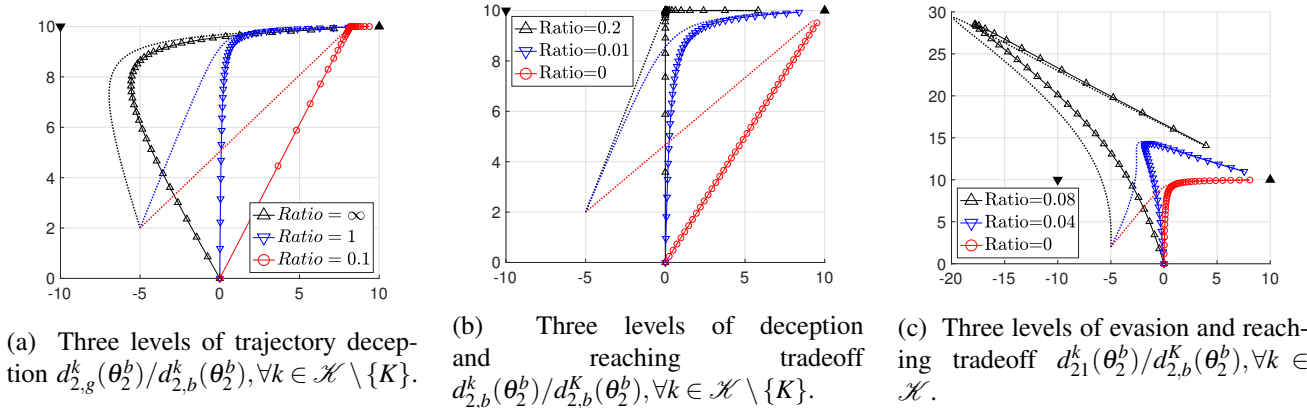


Fig. 2: The evader's trajectories with different initial locations shown in solid and the dashed lines, respectively.

Finally, we represent UAV i 's coupled cost g_i^k into the following matrix forms; i.e., $x_{d_1}^k(\theta_1) = \mathbf{0}_{4,1}, f_{d_1}^k(x_{d_1}^k(\theta_1)) = 0, F_{ii}^k(\theta_1) = f_{ii}^k(\theta_1) \cdot \mathbf{I}_2, F_{ij}^k(\theta_1) = -f_{ij}^k(\theta_1) \cdot \mathbf{I}_2, j \neq i, D_1^k(\theta_1) = d_1^k(\theta_1) \cdot [1, 0, -1, 0; 0, 1, 0, -1; -1, 0, 1, 0; 0, -1, 0, 1],$

$$D_2^k(\theta_2) = \begin{bmatrix} -d_{21}^k & 0 & d_{21}^k & 0 \\ 0 & -d_{21}^k & 0 & d_{21}^k \\ d_{21}^k & 0 & d_{2,b}^k + d_{2,g}^k - d_{21}^k & 0 \\ 0 & d_{21}^k & 0 & d_{2,b}^k + d_{2,g}^k - d_{21}^k \end{bmatrix},$$

$$x_{d_2}^k(\theta_2) = \frac{1}{d_{2,b}^k + d_{2,g}^k} [d_{2,b}^k x^b + d_{2,g}^k x^g; d_{2,b}^k y^b + d_{2,g}^k y^g; d_{2,b}^k x^b + d_{2,g}^k x^g; d_{2,b}^k y^b + d_{2,g}^k y^g], f_{d_2}^k(x_{d_2}^k(\theta_2)) = \frac{d_{2,b}^k d_{2,g}^k ((x^b - x^g)^2 + (y^b - y^g)^2)}{d_{2,b}^k + d_{2,g}^k}.$$

A. Finite-Horizon Analysis of Bayesian Update

Both the evader and the pursuer determine their initial beliefs based on the intelligence collected before their interaction. Then, they rely on the Bayesian update in (2) to obtain their beliefs at the following stages. In this subsection, we show that it is consistent, efficient, and robust for each player to adopt the finite-horizon Bayesian update to counter the opponent's deception. Define the belief of the high-maneuverability pursuer θ_1^H as $b^k := l_1^k(\theta_2^b | h^k, \theta_1^H)$, the likelihood function of θ_2^b as $a^k := \Pr(x^{k+1} | \theta_2^b, x^k, \theta_1^H)$, the likelihood function of θ_2^g as $c^k := \Pr(x^{k+1} | \theta_2^g, x^k, \theta_1^H)$. As $w^k \in \mathbb{R}^{n \times 1}$, a^k and c^k are always greater than 0. With an initial belief $b^0 \in (0, 1)$ and a finite likelihood ratio $e^k := c^k/a^k \in (0, \infty)$, (2) has the following closed form:

$$b^{k+1} = \frac{b^k \cdot a^k}{b^k \cdot a^k + (1 - b^k) \cdot c^k} = \frac{1}{1 + (\frac{1}{b^0} - 1) \prod_{k=0}^k e^k} \in (0, 1),$$

which results in the following properties.

- 1) **(Consistency:)** The belief change at stage k depends on the ratio e^k rather than the absolute value of a^k, c^k . In particular, if $e^k < 1$, then $b^{k+1} > b^k$; if $e^k > 1$, then $b^{k+1} < b^k$; if $e^k = 1$, then $b^{k+1} = b^k$.
- 2) **(Efficiency:)** If the evidence of state observation x^{k+1} suggests the type is more likely to be the true type θ_2^b , i.e., $e^k < 1$, then the function $b^{k+1}/b^k = 1/(b^k + (1 - b^k)e^k)$ at stage k is monotonically decreasing over b^k . If the evidence suggests the type is more likely to be the misleading type θ_2^g , i.e., $e^k > 1$, then the function b^{k+1}/b^k is monotonically increasing over b^k .

3) **(Robustness:)** The order of the evidence sequence $e^{\bar{k}}, \bar{k} = 0, \dots, k$, has no impact on the belief b^{k+1} .

Property one shows that although fluctuation can happen during the belief update due to the noise w^k , the belief mismatch, i.e., $1 - b^k$, will consistently decrease when $e^k < 1$, regardless of the prior belief $b^k \in (0, 1)$. Property two shows the efficiency of the belief update, i.e., the belief changes more under a large mismatch with the truth type. The above two properties are illustrated in Fig. 4 in the following subsection. Property three shows the robustness of the belief update. i.e., the heavy noise corruption which results in an erroneous belief update can be corrected later when the noise corruption is light.

B. Deceptive Evader with Decoupled Cost Structure

We first investigate the scenario where the evader has a decoupled cost structure defined in Definition 6; i.e., $d_{21}^k(\theta_2) = 0, \forall \theta_2 \in \Theta_2, \forall k \in \mathcal{K}$. According to Corollary 2, the evader's trajectory is then independent of the pursuer's action, type, and belief. The red line in Fig. 3 visualizes the evader's trajectory. Although the evader aims to keep his trajectory ambiguous throughout stages to prevent the pursuer from learning the true target, he starts to head toward the true target at around half of K stages so that he can reach the target in a cost-efficient fashion. If the evader chooses to head toward the target only in the last few stages, the distance between him and the true target will be large and he has to spend a huge control cost $(u_2^k)' F_{22}^k(\theta_2) u_2^k$ to reach the target. The pursuer's trajectory is shown via blue lines in Fig. 3. Although the pursuer only aims to be close to the evader at the final stage, she also takes proactive actions in the previous stages to be cost-efficient. If the pursuer knows the evader's type, then she can head toward the true target directly and will not be misled by the evader's trajectory ambiguity at the early stages. If the evader's type is private, then a larger initial belief mismatch $1 - l_1^0(\theta_2^b | x^0, \theta_1^H)$ makes the pursuer head more toward the misleading target at the early stages. However, due to the pursuer's online learning, she manages to approach the evader at the final stage regardless of the initial belief mismatch. Fig. 4 shows the pursuer's belief update over K stages. The evader's ambiguous trajectory results in belief fluctuations at the early stages, yet the pursuer can quickly reduce the belief mismatch when the evader starts to head toward the true target. Since we plot three belief variations under different initial beliefs with the same noise sequence w^k , they have the similar fluctuations before reaching the steady state. A video demo of two UAVs' trajectories and the belief update can be found at <http://bit.ly/Decoupled>.

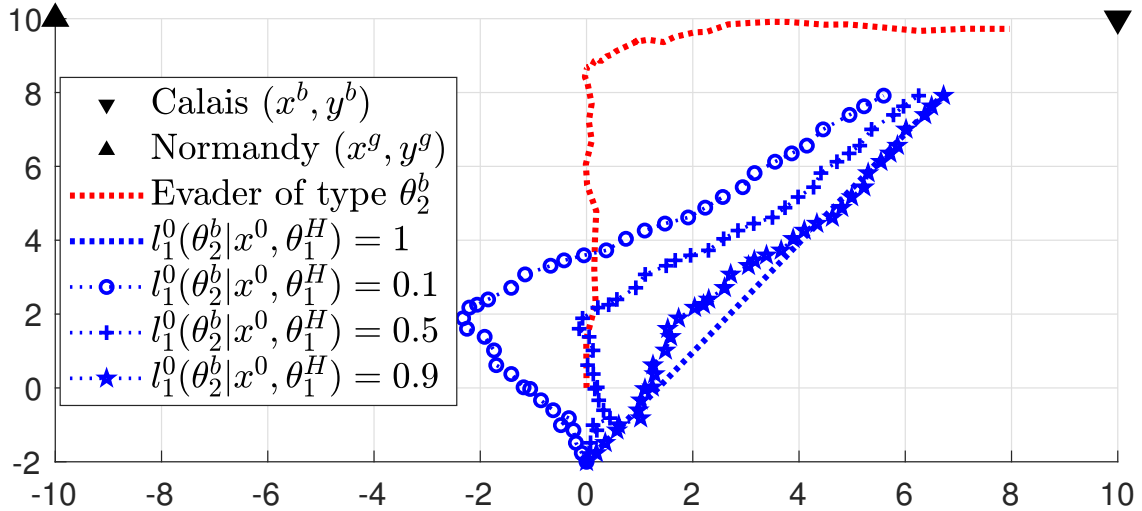


Fig. 3: The evader's and the pursuer's trajectories up to stage $K = 40$ in red and blue, respectively. The blue lines with markers represent the pursuer's trajectories under different initial beliefs l_1^0 and the one without markers represents a noise-free trajectory when the pursuer knows the evader's type.

1) **Comparison with Heuristic Policies:** We compare the proposed pursuer's strategy with two heuristic ones to demonstrate its efficiency in counting deception. The first heuristic policy is to repeat the attacker's trajectory with a one-stage delay; i.e., the pursuer applies the action so that $x_1^{k+1} = x_2^k, \forall k \in \mathcal{K} \setminus \{K\}$. The pursuer does not

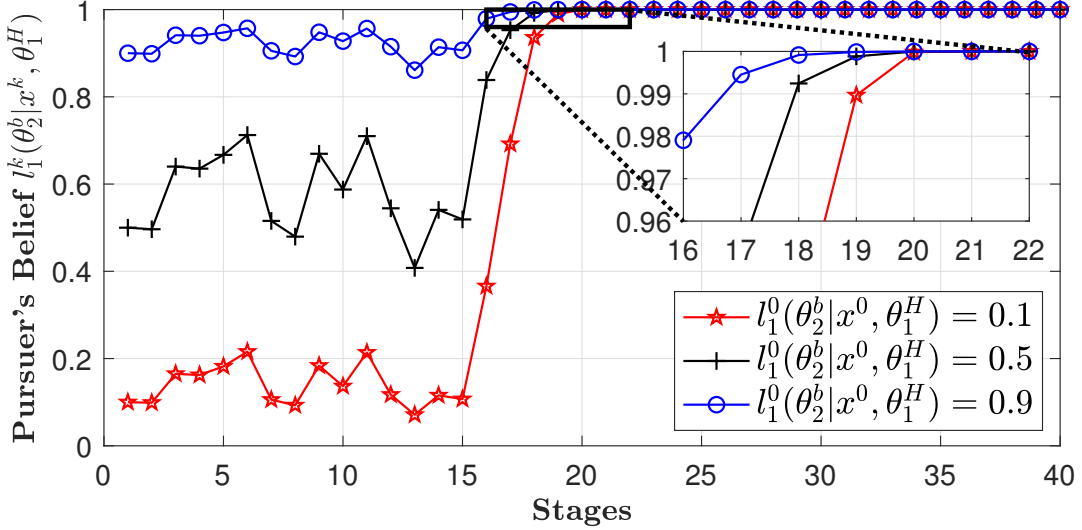


Fig. 4: The pursuer's K -stage belief variation under different initial beliefs l_1^0 and the same noise sequence $w^k, \forall k \in \mathcal{K}$. The black box magnifies the selected area.

need to apply Bayesian learning and we name this policy as *direct following*. The second heuristic policy for the pursuer is to stay at the initial location until her truth-revealing stage k_1^{tr} and then head toward the evader's expected final-stage location in the remaining stages. We call the second policy *conservative* because the pursuer does not take proactive actions until she has identified the evader's type. Although pursuers under both heuristic policies manage to stay close to the evader at the final stage, Fig. 5 shows that both heuristic policies result in much more costs than the proposed optimal strategy does over K stages.

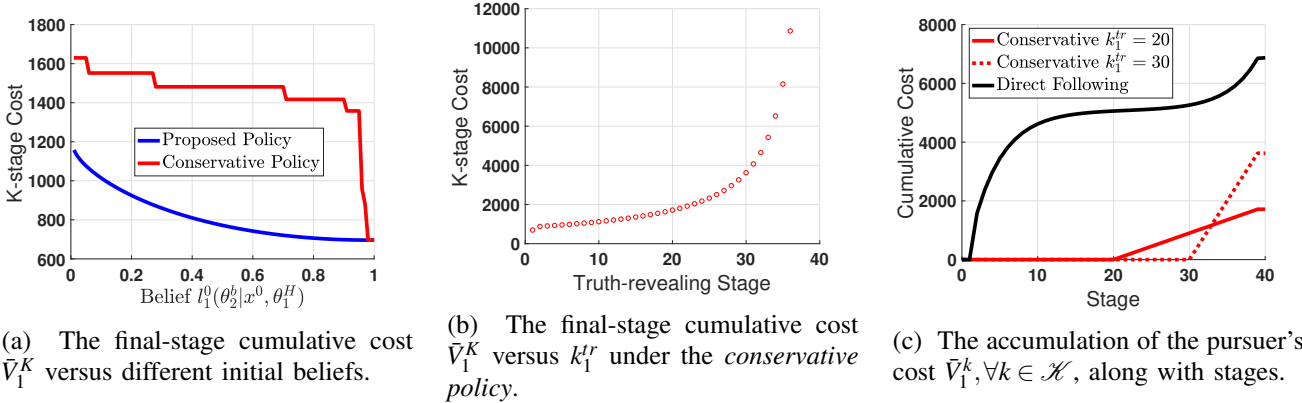


Fig. 5: The pursuer's cumulative cost under two heuristic policies and the proposed policy.

The conservative policy avoids potential trajectory deviations under deception but results in less planning stages for the pursuer to achieve the capture goal. We visualize the accumulation of the pursuer's cost \bar{V}_1^k in Fig. 5c. The red lines show that the pursuer who adopts *conservative policies* spends no action costs before the truth-revealing stage k_1^{tr} , i.e., $(u_1^k)'F_{11}^k(\theta_1)u_1^k = 0, \forall k \leq k_1^{tr}$, but huge costs in the remaining stages to fulfill her capture goal. The total cumulative cost \bar{V}_1^K at the final stage increases exponentially with the value of k_1^{tr} as shown in Fig. 5b. The black line in Fig. 5c illustrates the accumulation of \bar{V}_1^k when the pursuer direct follows the evader's trajectory. Only under extreme deception scenarios where $k_1^{tr} > 34$, the *direct following* policy results in a lower cost than the *conservative policies* does. Since the initial belief l_1^0 affects both the truth-revealing stage and the proposed policy, we plot \bar{V}_1^K versus l_1^0 under the *conservative policy* and the proposed policy in Fig. 5a. When there is no belief mismatch $l_1^0(\theta_2^b|x^0, \theta_1^H) = 1$, we have $k_1^{tr} = 1$ and the conservative policy is equivalent to the proposed policy. As

the belief mismatch increases, the cumulative cost \bar{V}_1^K under the proposed policy (resp. the conservative policy) increases due to the larger deviation along the x -axis (resp. the larger k_1^{tr}). The proposed policy always results in a lower cumulative cost \bar{V}_1^K than the conservative policy does. The results in Fig. 5 lead to the following two principles for the pursuer to behave under deception. First, Bayesian learning is a more effective countermeasure than a directly following of the evader's deceptive trajectory. Second, if learning the evader's type takes a long time, the pursuer is better to act proactively based on the current belief than to delay actions until the truth-revealing stage.

C. Dynamic Game for Deception and Counter-Deception

In this section, the evader has a coupled cost defined in Definition 6 and the level of *evasion determination* increases with a constant rate α ; i.e., $d_{21}^k(\theta_2) = \alpha k, \forall \theta_2 \in \Theta_2, \forall k \in \mathcal{K}$. We investigate the one-sided deception of the evader in Section IV-C1 and two-sided deception of both UAVs in Section IV-C2. A video demo of two UAVs' trajectories and their belief updates can be found at <http://bit.ly/CoupledCost>.

1) *Pursuer with a Public Type*: When the pursuer's type is common knowledge, we plot both UAVs' trajectories under two initial beliefs and two types of pursuers in Fig. 6. The red lines show that the evader with the coupled

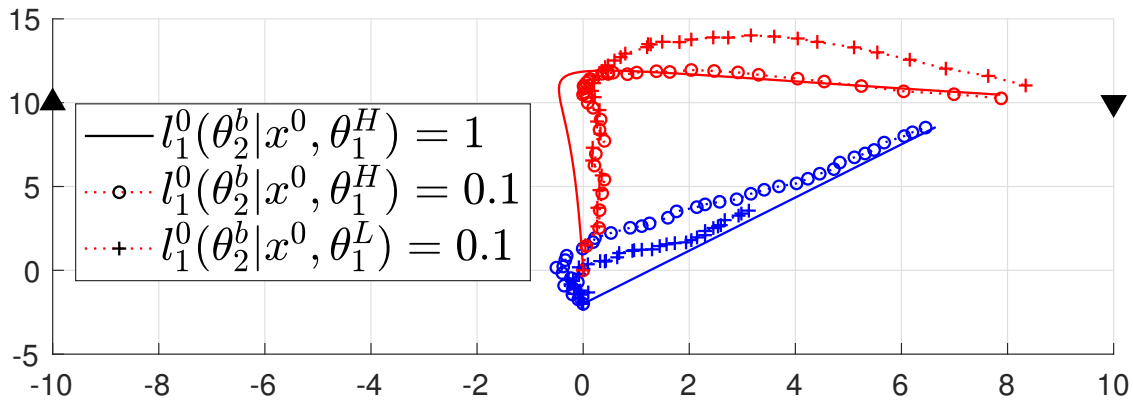


Fig. 6: The trajectory of the evader and the pursuer up to stage $K = 40$ in red and blue, respectively. If the evader's type is publicly known and the pursuer is of high-maneuverability, we represent their noise-free trajectories by the solid lines. If the evader's type is private and the pursuer's initial belief mismatch is 0.9, two UAVs' trajectories are denoted by dashed lines with circles (resp. plus signs) when the pursuer's maneuverability is high (resp. low).

cost detours to stay further from the pursuer. The initial belief mismatch causes a deviation along the x -axis for both high- and low-maneuverability pursuers as shown by the blue lines with circles and plus signs, respectively. However, the deviation has a smaller magnitude and lasts shorter than the one represented by the blue line with circles in Fig. 3 due to the coupled cost structure of the evader. The pursuer with a high maneuverability stays closer to the evader at the final stage.

2) *Deception for Counter-Deception*: When the pursuer's type is also private, Fig. 7 shows that she can manipulate the evader's initial belief l_2^0 to obtain a smaller k_1^{tr} and a belief update with less fluctuation. The red line with stars is the same as the one in Fig. 4. It shows that the pursuer's belief learning is slower and fluctuates more when she interacts with the evader who has a decoupled cost. The reason is that her manipulation of the initial belief l_2^0 does not affect the evader's decision making as shown in Corollary 2. A comparison between Fig. 7a and Fig. 7b shows that it is beneficial for a low-maneuverability pursuer to disguise as a high-maneuverability pursuer but not vice versa. Thus, applying deception to counter deception is not always effective.

D. Multi-Dimensional Deception Metrics

The impact of the evader's deception can be measured by various metrics such as the *endpoint distance* between the evader and the true target $x_2^{fd} := \|x_2^K - \gamma(\theta_2)\|_2$, the *endpoint distance* between two UAVs $x_1^{fd} := \|x_1^K - x_2^K\|_2$, both UAVs' truth-revealing stages k_i^{tr} , and their cumulative costs $\bar{V}_i^k, \forall k \in \mathcal{K}$. In this pursuit-evasion case study, we define the ε -reachability and ε -capturability in Definition 11. Although $x_i^{fd}, \forall i \in \{1, 2\}$, is a random variable,

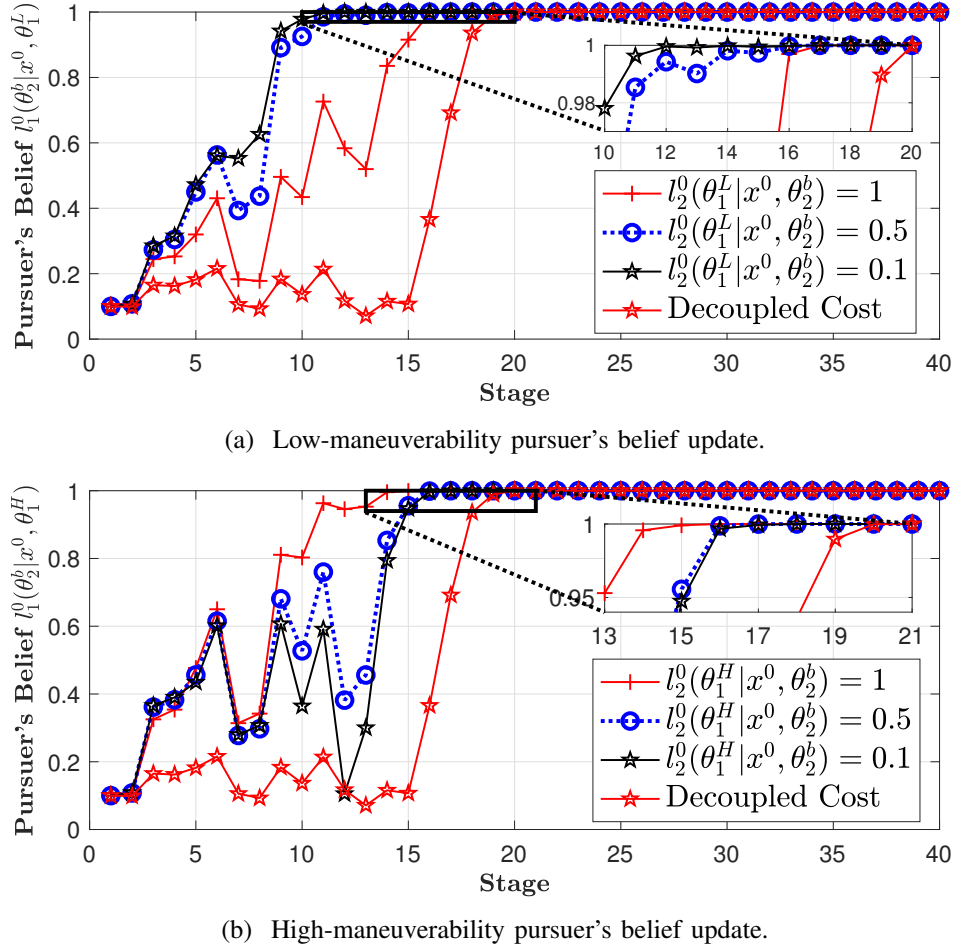


Fig. 7: The pursuer's belief update over K stages with the same initial belief $l_1^0(\theta_2^b | x^0, \theta_1) = 0.1$.

we can have a good estimate of the reachability and capturability due to the negligible variance of x_i^{fd} as shown in Fig. 8a and Fig. 9a.

Definition 11 (Reachability and Capturability). Consider the proposed pursuit-evasion scenario with a given $\varepsilon \geq 0$, a threshold $x_d^{fd} \geq 0$, and all initial beliefs $l_i^0 \in (0, 1)$. The target is ε -reachable if $\Pr(x_2^{fd} \geq x_d^{fd}) \leq \varepsilon$ and the evader is ε -capturable if $\Pr(x_1^{fd} \geq x_d^{fd}) \leq \varepsilon$.

In Section IV-D1, we investigate how the evader can manipulate the pursuer's initial belief $l_1^0(\theta_2^b | x^0, \theta_1^H)$ to influence the deception. In Section IV-D2, we investigate how the pursuer's maneuverability plays a role in deception. In both sections, the evader has a coupled cost structure. The pursuer either applies the Bayesian update or not, which is denoted by blue and red lines, respectively, in both Fig. 8 and Fig. 9.

1) *The Impact of the Evader's Belief Manipulation:* Both UAVs determine their initial beliefs based on the intelligence collected before their interactions. By falsifying the pursuer's intelligence, the evader can manipulate the pursuer's initial belief l_1^0 and further influence the deception as shown in Fig. 8. In the x -axis, an initial belief $l_1^0(\theta_2^b | x^0, \theta_1^H)$ closer to 1 indicates a smaller belief mismatch. Fig. 8a shows that the pursuer's distance to the evader at the final stage decreases as the belief mismatch decreases regardless of the existence of Bayesian learning. However, the initial belief manipulation has a much less influence on the endpoint distance x_1^{fd} when Bayesian learning is applied. Fig. 8b shows that for each realization of the noise sequence w^k , the pursuer's truth-revealing stage steps down as the belief mismatch decreases when Bayesian update is applied. Fig. 8c illustrates the pursuer's cumulative cost \bar{V}_1^K and \bar{V}_1^{K-1} at the last and the second last stage, respectively. Without Bayesian update, the evader's deception incurs a huge cost increase to the pursuer at the second last stage due to the large endpoint distance x_1^{fd} . The red lines show that the cost increase is higher under a larger belief mismatch. Fig. 8d illustrates

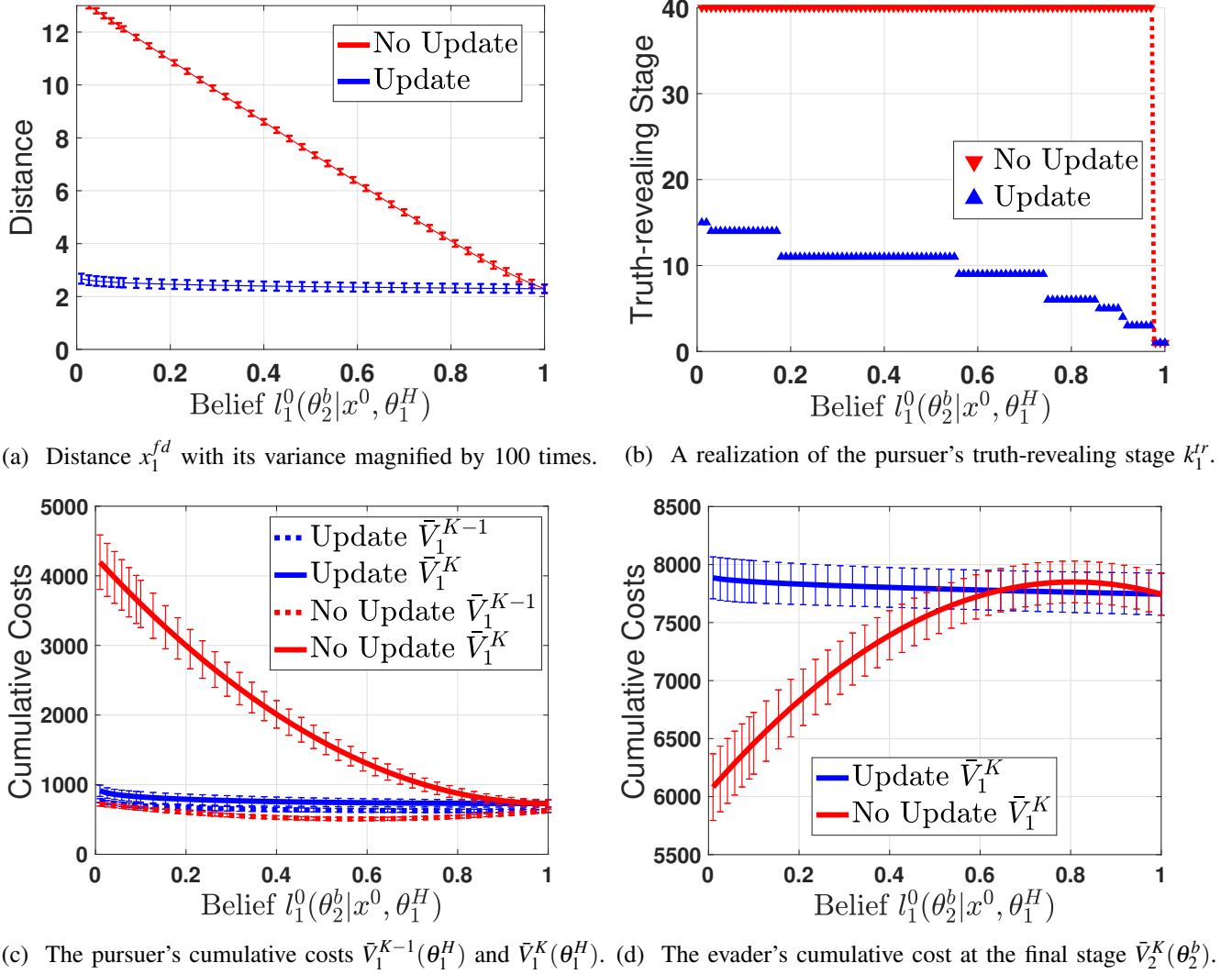


Fig. 8: The influence of the initial belief mismatch on deception. Error bars represent variances of the random variables.

the evader's cumulative cost at the last stage. If the pursuer does not apply Bayesian learning, then the evader can decrease his cost by increasing the pursuer's belief mismatch. If the pursuer applies Bayesian learning, then the evader's cost increases slightly if the pursuer's belief mismatch is increased. When the belief mismatch is small (i.e., $1 - l_1^0 \in (0, 0.35)$), we observe a win-win situation; i.e., Bayesian learning not only reduces the pursuer's cumulative cost, but also the evader's.

2) *The Impact of the Pursuer's Maneuverability*: The pursuer's maneuverability can also affect deception as shown in Fig. 9. The pursuer has an initial belief $l_1^0(\theta_2^b|x^0, \theta_1^H) = 0.5$ and the evader knows the pursuer's type. Fig. 9a illustrates that the pursuer can exponentially decrease her distance to the evader at the final stage as her maneuverability increases. Fig. 9b demonstrates that the maneuverability increase can decrease and increase the pursuer's and the evader's cumulative cost at the final stage, respectively. The variance grows as maneuverability decreases because the pursuer's trajectory will become largely affected by the external noise. In both figures, we observe the phenomenon of *marginal effect*; i.e., the change rates of both the endpoint distance x_1^{fd} and the cumulative cost \bar{V}_i^K decrease as the maneuverability increases. Thus, we conclude that higher maneuverability can improve the pursuer's counter-deception performance measured by the distance x_1^{fd} and the cost \bar{V}_1^K . Moreover, the improvement rate is higher when the maneuverability is low.

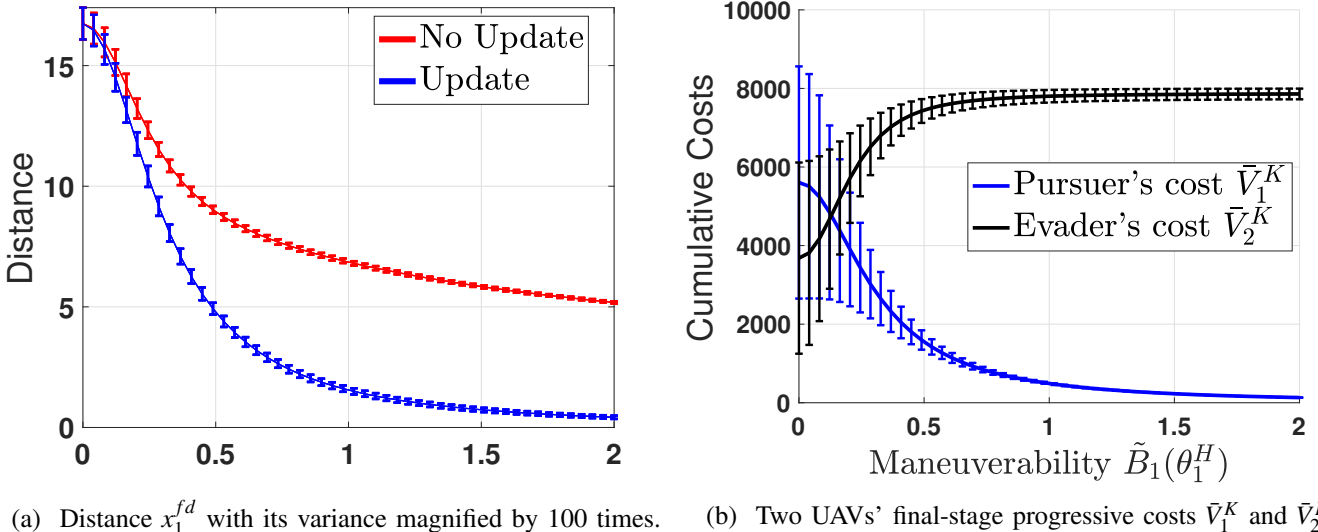


Fig. 9: The influence of the pursuer's maneuverability on deception. Error bars represent variances of the random variables.

3) *Deceivability, Distinguishability, and PoD*: Deceivability defined in Definition 9 is highly related to the distinguishability among different types. In this case study, a larger distance between targets, i.e., $\|\gamma(\theta_2^g) - \gamma(\theta_2^b)\|_2$, makes it easier for the pursuer to distinguish evaders of type θ_2^b and θ_2^g . A larger maneuverability difference $|\tilde{B}_1(\theta_1^H) - \tilde{B}_1(\theta_1^L)|$ makes it easier for the evader to distinguish pursuers of type θ_1^H and θ_1^L . We visualize two UAVs' truth-revealing stages k_i^{tr} versus the distance between targets and the maneuverability difference in Fig. 10. The evader has a coupled cost and both players' initial belief mismatch is 0.5. The dashed black line indicates $\tilde{B}_1(\theta_1^L) = 0.3$. When the maneuverability difference is negligible $\tilde{B}_1(\theta_1^H) \in (0.26, 0.36)$, the pursuer's type cannot be learned correctly in K stages; i.e., the pursuer is $(K+1)$ -stage 0-deceivable. When the maneuverability difference is small, i.e., $\tilde{B}_1(\theta_1^H) \in (0.1, 0.5)$ yet not negligible, i.e., $\tilde{B}_1(\theta_1^H) \notin (0.26, 0.36)$, the variance of k_2^{tr} is large.

We choose $\eta_1 = \eta_2 = 0.5$ and visualize the PoD in Fig. 11. The numerical results corroborate that the PoD can be bigger than 1 and has a negligibly small variance even though the variance of \bar{V}_i^K is large as shown in Fig. 8c, Fig. 8d, and Fig. 9b. Besides, the PoD does not change much as the initial belief l_1^0 and the maneuverability change.

V. CONCLUSION

We have investigated a novel class of *rational robot deception* problems where intelligent robots hide their heterogeneous private information to achieve their objectives in finite stages with minimum costs. We have proposed a nonzero-sum dynamic game framework to quantify the impact of deception and design long-term optimal actions for deception and counter-deception. Robots form their own initial beliefs on others' private information and use Bayesian update to reduce their belief mismatches. Satisfying the properties of sequential rationality and belief consistency, level-t Bayesian Nash equilibrium can be used to compute N robots' actions and beliefs over the K stages. We have studied a class of games in the linear-quadratic form to obtain an explicit state-feedback control policy and a set of extended Riccati equations. The concepts of deceivability and distinguishability have been defined to characterize the fundamental limits of deception. Meanwhile, the concepts of reachability and capturability characterize the performance limit under deception. The concept of the price of deception serves as a crucial evaluation and design metric for different robot deception scenarios.

We have investigated a case study of dynamic target protection where the evader aims to deceptively reach the target and the pursuer keeps her maneuverability as private information. The pursuer has the lowest cumulative cost under the proposed policy than the direct-following and conservative policies. We have proposed multi-dimensional metrics such as the stage of truth revelation, the endpoint distance, and the cumulative cost to measure the deception impact throughout stages. We have concluded that Bayesian learning can largely reduce the impact of initial belief

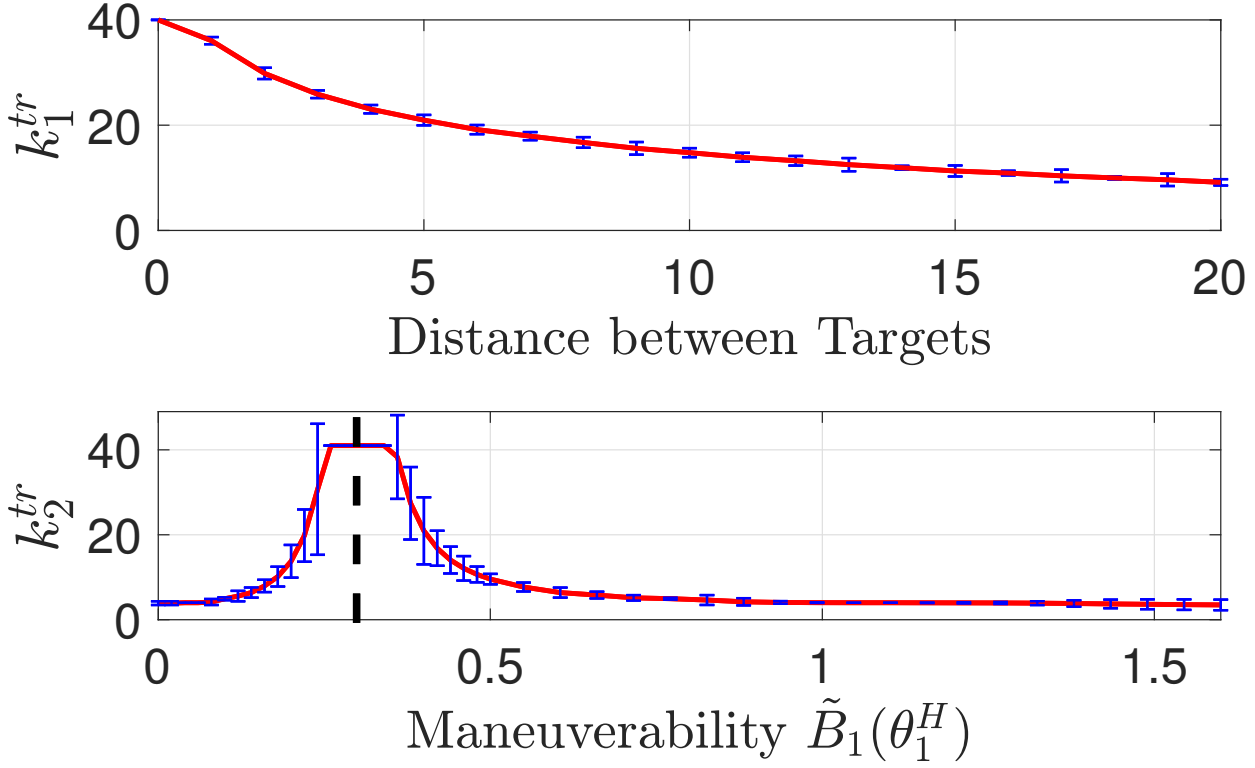


Fig. 10: The plot of the deceived robot's truth-revealing stage versus the deceiver's type distinguishability. Error bars represent their variances, which are magnified by 5 times.

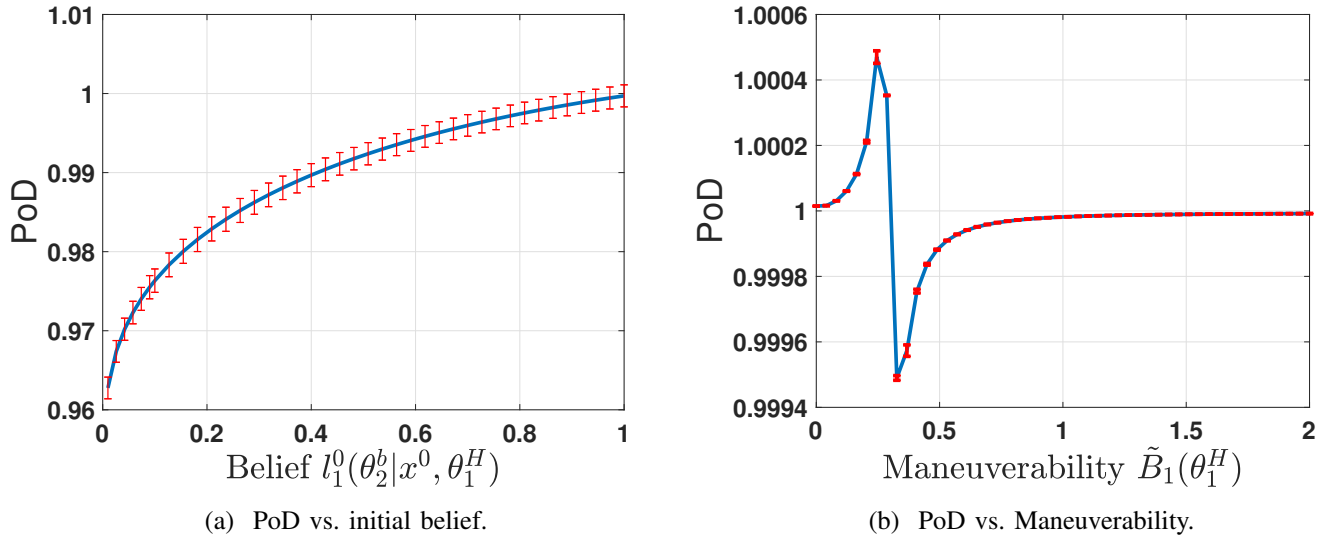


Fig. 11: The price of deception p_d . Error bars represent p_d 's variances which are magnified by 1000 times.

manipulation and sometimes result in a win-win situation. The increase of the pursuer's maneuverability can also reduce the endpoint distance and her cumulative cost yet has a marginal effect. A robot is more deceivable, i.e., less learnable when his/her potential types are less distinguishable. Finally, we have found that the idea of using deception to counter deception is not always effective. In particular, it is beneficial for the low-maneuverability pursuer to disguise as a high-maneuverability pursuer but not vice versa.

REFERENCES

- [1] D. L. Smith, *Why we lie: The evolutionary roots of deception and the unconscious mind*. Macmillan, 2004.
- [2] M. Howard and M. E. Howard, *Strategic Deception in the Second World War*. WW Norton & Company, 1995, vol. 5.
- [3] L. Cowen, T. Ideker, B. J. Raphael, and R. Sharan, "Network propagation: a universal amplifier of genetic associations," *Nature Reviews Genetics*, vol. 18, no. 9, p. 551, 2017.
- [4] E. Al-Shaer, J. Wei, K. W. Hamlen, and C. Wang, "Dynamic bayesian games for adversarial and defensive cyber deception," in *Autonomous Cyber Deception*. Springer, 2019, pp. 75–97.
- [5] D. Li and J. B. Cruz, "Defending an asset: a linear quadratic game approach," *IEEE Transactions on Aerospace and Electronic Systems*, vol. 47, no. 2, pp. 1026–1044, 2011.
- [6] H. Hajieghrary, D. Kularatne, and M. A. Hsieh, "Cooperative transport of a buoyant load: A differential geometric approach," in *2017 IEEE/RSJ International Conference on Intelligent Robots and Systems (IROS)*. IEEE, 2017, pp. 2158–2163.
- [7] K. Sreenath and V. Kumar, "Dynamics, control and planning for cooperative manipulation of payloads suspended by cables from multiple quadrotor robots," *rn*, vol. 1, no. r2, p. r3, 2013.
- [8] J. C. Harsanyi, "Games with incomplete information played by bayesian players, i–iii part i. the basic model," *Management science*, vol. 14, no. 3, pp. 159–182, 1967.
- [9] V. L. Thing and J. Wu, "Autonomous vehicle security: A taxonomy of attacks and defences," in *2016 IEEE International Conference on Internet of Things (iThings) and IEEE Green Computing and Communications (GreenCom) and IEEE Cyber, Physical and Social Computing (CPSCom) and IEEE Smart Data (SmartData)*. IEEE, 2016, pp. 164–170.
- [10] Y. Huang, J. Chen, L. Huang, and Q. Zhu, "Dynamic games for secure and resilient control system design," *National Science Review*.
- [11] Y. Zhao, L. Huang, C. Smidts, and Q. Zhu, "Finite-horizon semi-markov game for time-sensitive attack response and probabilistic risk assessment in nuclear power plants," *Reliability Engineering & System Safety*, p. 106878, 2020.
- [12] N. Bezzo, J. Weimer, M. Pajic, O. Sokolsky, G. J. Pappas, and I. Lee, "Attack resilient state estimation for autonomous robotic systems," in *2014 IEEE/RSJ International Conference on Intelligent Robots and Systems*. IEEE, 2014, pp. 3692–3698.
- [13] S. Bhattacharya and T. Başar, "Game-theoretic analysis of an aerial jamming attack on a uav communication network," in *Proceedings of the 2010 American Control Conference*. IEEE, 2010, pp. 818–823.
- [14] R. Zhang and P. Venkitasubramaniam, "Stealthy control signal attacks in linear quadratic gaussian control systems: detectability reward tradeoff," *IEEE Transactions on Information Forensics and Security*, vol. 12, no. 7, pp. 1555–1570, 2017.
- [15] A. Ayub, A. Morales, and A. Banerjee, "An adaptive markov process for robot deception," *arXiv preprint arXiv:1910.10251*, 2019.
- [16] M. Ornik and U. Topcu, "Deception in optimal control," in *2018 56th Annual Allerton Conference on Communication, Control, and Computing (Allerton)*. IEEE, 2018, pp. 821–828.
- [17] B. R. Brewer, R. L. Klatzky, and Y. Matsuoka, "Visual-feedback distortion in a robotic rehabilitation environment," *Proceedings of the IEEE*, vol. 94, no. 9, pp. 1739–1751, 2006.
- [18] J. Shim and R. C. Arkin, "Other-oriented robot deception: A computational approach for deceptive action generation to benefit the mark," in *2014 IEEE International Conference on Robotics and Biomimetics (ROBIO 2014)*. IEEE, 2014, pp. 528–535.
- [19] A. D. Dragan, R. M. Holladay, and S. S. Srinivasa, "An analysis of deceptive robot motion," in *Robotics: science and systems*. Citeseer, 2014, p. 10.
- [20] J. Shim and R. C. Arkin, "A taxonomy of robot deception and its benefits in hri," in *2013 IEEE International Conference on Systems, Man, and Cybernetics*. IEEE, 2013, pp. 2328–2335.
- [21] A. R. Wagner and R. C. Arkin, "Acting deceptively: Providing robots with the capacity for deception," *International Journal of Social Robotics*, vol. 3, no. 1, pp. 5–26, 2011.
- [22] P. G. Bennett, "Hypergames: developing a model of conflict," *Futures*, vol. 12, no. 6, pp. 489–507, 1980.
- [23] J. Pawlick and Q. Zhu, "Deception by design: evidence-based signaling games for network defense," *arXiv preprint arXiv:1503.05458*, 2015.
- [24] L. Huang and Q. Zhu, "A dynamic games approach to proactive defense strategies against advanced persistent threats in cyber-physical systems," *Computers & Security*, vol. 89, p. 101660, 2020.
- [25] K. Horák, Q. Zhu, and B. Bošanský, "Manipulating adversarys belief: A dynamic game approach to deception by design for proactive network security," in *International Conference on Decision and Game Theory for Security*. Springer, 2017, pp. 273–294.
- [26] F. Miao, Q. Zhu, M. Pajic, and G. J. Pappas, "A hybrid stochastic game for secure control of cyber-physical systems," *Automatica*, vol. 93, pp. 55–63, 2018.
- [27] F. Miao and Q. Zhu, "A moving-horizon hybrid stochastic game for secure control of cyber-physical systems," in *53rd IEEE Conference on Decision and Control*. IEEE, 2014, pp. 517–522.
- [28] J. Cruz, M. A. Simaan, A. Gacic, and Y. Liu, "Moving horizon nash strategies for a military air operation," *IEEE Transactions on Aerospace and Electronic Systems*, vol. 38, no. 3, pp. 989–999, 2002.
- [29] A. Liniger and J. Lygeros, "A noncooperative game approach to autonomous racing," *IEEE Transactions on Control Systems Technology*, 2019.
- [30] N. Sandell and M. Athans, "Solution of some nonclassical lqg stochastic decision problems," *IEEE Transactions on Automatic Control*, vol. 19, no. 2, pp. 108–116, 1974.
- [31] E. Maskin and J. Tirole, "Markov perfect equilibrium: I. observable actions," *Journal of Economic Theory*, vol. 100, no. 2, pp. 191–219, 2001.
- [32] J. W. Clemens and J. L. Speyer, "On the lqg game with nonclassical information pattern using a direct solution method," *IEEE Transactions on Automatic Control*, 2019.
- [33] A. Gupta, A. Nayyar, C. Langbort, and T. Basar, "Common information based markov perfect equilibria for linear-gaussian games with asymmetric information," *SIAM Journal on Control and Optimization*, vol. 52, no. 5, pp. 3228–3260, 2014.
- [34] Y. Ouyang, H. Tavafoghi, and D. Tenekezis, "Dynamic games with asymmetric information: Common information based perfect bayesian equilibria and sequential decomposition," *IEEE Transactions on Automatic Control*, vol. 62, no. 1, pp. 222–237, 2016.

- [35] D. Vasal and A. Anastasopoulos, "Signaling equilibria for dynamic lqg games with asymmetric information," in *2016 IEEE 55th Conference on Decision and Control (CDC)*. IEEE, 2016, pp. 6901–6908.
- [36] A. Nayyar, A. Mahajan, and D. Teneketzis, "The common-information approach to decentralized stochastic control," in *Information and Control in Networks*. Springer, 2014, pp. 123–156.
- [37] D. Fudenberg and J. Tirole, *Game Theory*. Cambridge, MA: MIT Press, 1991, translated into Chinesse by Renin University Press, Bejing: China.
- [38] O. L. V. Costa, M. D. Fragoso, and R. P. Marques, *Discrete-time Markov jump linear systems*. Springer Science & Business Media, 2006.
- [39] A. Doucet, A. Logothetis, and V. Krishnamurthy, "State estimation of jump markov linear systems via stochastic sampling algorithms," in *Proceedings of the 37th IEEE Conference on Decision and Control (Cat. No. 98CH36171)*, vol. 2. IEEE, 1998, pp. 2305–2310.
- [40] A. Doucet, N. J. Gordon, and V. Krishnamurthy, "Particle filters for state estimation of jump markov linear systems," *IEEE Transactions on signal processing*, vol. 49, no. 3, pp. 613–624, 2001.
- [41] T. Basar and G. J. Olsder, *Dynamic noncooperative game theory*. Siam, 1999, vol. 23.
- [42] D. Fridovich-Keil, V. Rubies-Royo, and C. J. Tomlin, "An iterative quadratic method for general-sum differential games with feedback linearizable dynamics," *arXiv preprint arXiv:1910.00681*, 2019.
- [43] L. Huang and Q. Zhu, "Analysis and computation of adaptive defense strategies against advanced persistent threats for cyber-physical systems," in *International Conference on Decision and Game Theory for Security*. Springer, 2018, pp. 205–226.
- [44] ——, "Adaptive strategic cyber defense for advanced persistent threats in critical infrastructure networks," *ACM SIGMETRICS Performance Evaluation Review*, vol. 46, no. 2, pp. 52–56, 2019.